2.03 Fuel Performance of Fast Spectrum Oxide Fuel[☆]

Michel Pelletier and Yannick Guérin, CEA, DES, IRESNE, DEC, Cadarache F-13108, Saint-Paul-Lez-Durance, France

[☆]*Change History*: July 2019. Michel Pelletier and Yannick Guérin has added two sub-chapters at the end before the general conclusion. They deal with the concept of fuel pin with annular shaped pellets and with the concept of axial heterogeneous fuel pin (Ax-Het). A number of corrections or clarifications have been made compared to the original text written by Yannick Guérin. In particular the data of Table 1 have been updated and some figures improved. In addition new references of articles published since 2012 have been added.
This is an update of Guerin, Y., 2012. Chapter 2.21 – Fuel Performance of Fast Spectrum Oxide Fuel. In: Konings, R.J.M. (Ed.), Comprehensive Nuclear Materials, Elsevier, pp. 547–578.

 doi:10.1016/B978-0-12-803581-8.11690-X

Nomenclature

c Plutonium concentration (m^{-3})
D Diffusion rate of plutonium (m^{-2})
E Young's modulus (GPa)
h Heat transfer coefficient (W m^{-2} K^{-2})
$\mathbf{J_{Pu}}$ Flux of plutonium (m^{-2} s^{-1})
$\mathbf{P_l}$ Linear Heat Rate (W cm^{-1})
Q* Heat of transport (J K^{-1})
r Radius (m)
R Gas constant (J K^{-1} mol^{-1})
T Temperature (K)
$\mathbf{V_i}$ Atomic volume of atom (i) ($m^{3)}$
$\mathbf{V_{Pu}}$ Atomic volume of plutonium (m^3)
x O/M ratio deviation (/)
α Thermal expansion coefficient (K^{-1})
$\mathbf{\Delta H_v}$ Vaporization enthalpy (J)
ϕ Neutron flux (n cm^{-2} s^{-1})
λ Thermal conductivity (W m^{-1} K^{-1})
ν Poisson's ratio (/)
σ Stress (MPa)

Glossary

Ax-Het Axially heterogeneous (core or fuel pin)
CW Cold worked
DND Delayed neutron detector
dpa displacement per atom
DRF Dounreay fast reactor (UK)
EFR European fast reactor
EPMA Electron probe microAnalysis
FCCI Fuel cladding chemical interaction
FCMI Fuel cladding mechanical interaction
FFTF Fast flux test facility
FP Fission product
HBS High burnup structure
JOG Joint oxyde gaine (oxide cladding joint)
LBE Lead bismuth eutectic
LHR Linear heat rate
LWR Light water reactor
MA Minor actinides
NTP Normal temperature and pressure
O/M ratio Oxygen to metal ratio
ODS Oxide dispersion strengthened
PFR Prototype fast reactor (Dounreay UK)
PWR Pressurized water reactor
R&D Research and development
RE Rare earth metal (or lanthanide)
SA Solution annealed
SEM Scanning electron microscope
SFR Sodium fast reactor
TD Theoretical density

2.03.1 Introduction

Despite some disadvantages, such as its low density of heavy atoms, its poor thermal conductivity, and its chemical reaction with sodium, mixed oxide fuel $(U,Pu)O_2$ is the fuel that has been used most in sodium fast reactors (SFR) worldwide. This is due to its advantageous properties such as high melting point, with no allotropic changes, excellent stability, and an excellent behavior under irradiation, in particular, a swelling rate much lower than the other fuels.

Oxide fuel is contemplated as a reference fuel in several fast reactor systems of Generation IV, in particular, sodium-cooled fast reactors and LBE (lead bismuth eutectic)-cooled reactors. Nevertheless, experience on the behavior of oxide fast fuel has been gained essentially in sodium fast reactors and, consequently, this article addresses mainly this type of fuel.

This article recalls first some generalities on fast oxide fuels: existing experience, main design of fuel pins, operating conditions, requirements, and main objectives of fuel development. Then, the main phenomena occurring in fast oxide fuels are described, focusing first on behavior at the beginning of life and high-temperature effects such as fuel restructuring, radial redistribution of fuel constituents, and geometrical evolution. The behavior of fission products is described, with the consequences on thermochemistry of oxide pellets such as the evolution of O/M ratio, as well as on fuel swelling or fission gas release. The main potential-limiting phenomena are presented, addressing thermal, mechanical, and chemical life-limiting mechanisms. The behavior of in-pile failed pins is briefly recalled before concluding the article.

General information on fast oxide fuel behavior and performance can also be found in Olander,[1] Lambert,[2] Guérin,[3] Millet,[4] Martin,[5] and Pelletier.[6]

2.03.2 Experience With Oxide Fuels in Fast Reactors

2.03.2.1 History of Development

The first fast breeder reactors, built in the 1950s in the United States and in the United Kingdom, used metallic fuel (plutonium and uranium), as metals offer the highest heavy metal density and therefore the highest breeding ratio. Because of dimensional instability due to swelling and growth, metal fuels could hardly achieve high burnup. By the 1960s, mixed uranium and plutonium oxide $(U,Pu)O_2$ was known to be highly radiation tolerant and began to be considered as a reference fuel for fast reactors. Extensive studies were also carried out on mixed carbide and nitride fuels (U,Pu)C and (U,Pu)N, which have a better breeding ratio than oxide, thanks to their density, which lies between the oxide and the metal fuel.

The experimental fast reactor built in the 1960s and 1970s largely used mixed oxide as a reference fuel. This was the case in Rapsodie (France, 1967), BOR 60 (Russian Federation, 1968), KNK II (Germany, 1972), Joyo (Japan, 1978), and FFTF (USA, 1980). As irradiation of oxide fuels in these reactors was highly successful, all the prototype or commercial fast reactors built in the 1970s later chose oxide as reference fuels (**Table 1**).

As a result, mixed oxide is the fuel of which experience is by far the largest available. Several hundreds of thousands of oxide fuel pins have been successfully irradiated worldwide in fast reactors (e.g., 180,000 in Phénix, 98,000 in Prototype Fast Reactor (PFR), 63,000 in FFTF). Along with driver fuels, a great number of experimental fuel pins have been irradiated, in order either to test new fuel pin designs or new cladding materials, or in order to test behavior in off-normal conditions, including accidental

Table 1 Main characteristics of standard fuel pins irradiated in the prototype and commercial sodium fast reactors (P > 200 MWth) [IWGFR 1991, IAEA-TECDOC 2006]

	BN350	*Phénix*	*PFR*	*BN600*	*FFTF*[a]	*Super-Phénix*	*Monju*
First criticality	1972	1973	1974	1980	1980	1985	1994
Thermal Power (MWth)	750	563	600	1470	400	2990	714
Electric Power (MWe)	350[b]	250	250	600	/	1242	280
Type of fuel	UO_2	$(U,Pu)O_2$	$(U,Pu)O_2$	UO_2	$(U,Pu)O_2$	$(U,Pu)O_2$	$(U,Pu)O_2$
Number of subassemblies (inner/outer core)	109/113	55/48	28/44	230/139	28/45	193/171	108/90
Number of pins per assembly	127	217	325	127	217	271	169
Type of spacer	wire	wire	grids	wire	wire	wire	wire
Length of pin (m)	1.800	1.793	2.250	2.445	2.380	2.700	2.813
Height of fissile column (m)	1.060	0.850	0.914	1.000	0.914	1.000	0.930
Lower fertile column length (m)	0.400	0.300	0.450	0.400	/	0.300	0.350
Upper fertile column length (m)	0.570	0.31	0.45	0.40	/	0.30	0.30
Clad outer diameter (mm)	6.90	6.55	5.80	6.90	5.84	8.50	6.50
Clad thickness (mm)	0.40	0.45	0.38	0.40	0.38	0.565	0.47
Helical wire diameter (mm)		1.15			1.42	1.2	1.32
Pellet diameter (mm)		5.42				7.14	5.4
Fuel clad diametral gap (mm)		0.23			0.14	0.23	0.16
Central hole diameter (mm)	0	0	1.5	0		2.0	0
Fissile atoms / (U + Pu) (%) (inner core/outer core)	17/26	18/23	22/28	17/26	20/25	15/22	16/21
Fuel density (% TD)	95	95.5	97	95	90.4	95.5	85
Smeared density (% TD)	75	88	78	77	86	83	80
Plenum volume (cm^3)	8	13	14	21	19	43	28
Max. Linear Heat Rate (W/cm)	400	450	420	472	413	470	360
Peak cladding temperature (°C)	570	650	670	700	660	620	675
Max. neutron flux (10^{15} n.cm^2/s)	5.4	7.3	7.6	6.5	7	6.1	6.0
Maximum burnup (at%) (GWd/t of HM)	10.0	16.9	23.5	11.8	24.5	Not relevant	Not relevant
	97	160	220	113			
Maximum dose (dpa NRT)	60	156	155	90		/	/

[a]FFTF is usually classified as an experimental reactor rather than a prototype reactor. But from a fuel point of view, irradiation of fuel pins in FFTF is rather prototypic.
[b]Including 200 MWe for desalting water.

situations. All of these experiments provided a solid background of knowledge on the behavior of oxide fuel and a large database for the validation of models and fuel performance codes.

2.03.2.2 Fuel Element Design

Table 1 provides the main characteristics of fuel elements in a certain number of prototype and commercial fast reactors. Despite the scatter in the values of the different parameters, these fuel elements refer to rather similar fuel concepts.

The fuel pin is a long cylinder (2–3 m long, 5–10 mm diameter), clad in a steel tube (~0.4–0.6 mm thick) closed in both ends by welded plugs, preventing direct contact between the radioactive material and the sodium coolant. The cladding serves as a first safety barrier and is designed to keep its integrity and tightness in nominal and off-normal conditions.

The oxide fissile column (~1 m long) consists of a stack of conventionally pressed and sintered pellets with an outer diameter slightly smaller than the inner diameter of the clad, providing a gap (~100 μm radial gap) between fuel and cladding needed for the fabrication. Depending upon the design, both full pellets and annular pellets (with a central hole between 1.5 and 2 mm) have been used. Other concepts have also been tested (especially in United Kingdom and Russia), where pellets are replaced by a vibropacked piling-up of fuel particles, which may be either spheres produced by sol–gel, or fuel particles obtained by a pyrometallurgical process. (In the pyrometallurgical process, spent fuel is dissolved in molten salt and oxide is extracted by electrolysis.)

UO_2 axial blankets (0.3–0.5 m long) made with natural or depleted uranium are placed at the lower and upper ends of the fissile column. The presence and geometry of such blankets depends on the degree of breeding capacity wanted. But, other concepts of fuel pins have also been tested, as the axially heterogeneous fuel pin (Ax-Het concept – see Section 2.03.7.2) in which a short fertile column (~ 0.2 m long) is located in the middle of the fissile column, in order to decrease the reactivity loss rate.[7]

Two gas plenums are located at both ends of the fuel pin, providing free volume for the released fission gases and limiting the internal pressure induced by fission gas release. Typically, the volumes of the plena and of the fissile column are about the same. The largest plenum is preferably located at the bottom end of the fuel pin, as it is the colder place in the fuel pin, thus mitigating the gas pressure increase. At the end of fabrication, fuel pins contain helium gas under 1 atm. Helium has been chosen because of its high thermal conductivity in order to improve the heat transfer through the gap between the fuel and the cladding at the beginning of life. In the upper plenum, a stainless steel spring maintains the fuel column during fabrication, transportation, and handling stages before irradiation.

Fuel subassemblies consist of a bundle of hexagonally packed fuel pins (~ 100–350 pins in each subassembly).

Around each pin, a steel wire (~ 1–1.5 mm diameter), made with the same type of material as the cladding, helically wrapped and welded or crimped to the end plugs, ensures regular spacing of the pins and sodium mixing. In some reactors, such as PFR and KNK II, grids replace the helical wire and ensure the spacing function.

Parallel rails make up a bottom grid to which the lower plugs of fuel pins are attached.

The bundle of fuel pins is contained in a steel hexagonal wrapper tube, which has essentially two functions: it forms the cooling channel and allows coolant flow to be adjusted, thanks to a depressor system located in the bottom nozzle. With the top and the bottom nozzle to which it is connected by welding and crimping, it forms the mechanical structure of the subassembly, allowing handling and positioning in the reactor core.

The core of the reactor consists of a compact hexagonal arrangement of a great number of subassemblies (~ 100–400).

The diameter of the core is about 1–2 m in prototypic reactors, up to 4 m in commercial reactor. The core is typically 1 m high, or a little less in prototypic reactors.

Fuel pellets are generally mixed oxide $(U,Pu)O_2$ (with the exception of Russian reactors where they are made of enriched UO_2) with a plutonium content between 15% and 30%. The plutonium content is higher in the outer core than in the inner core in order to compensate the decrease of neutron flux at the periphery of the reactor core.

The oxide pellets, fabricated by powder metallurgy (ball milling, pressing, and sintering), contain several volume percentages of porosity that will help accommodate fuel swelling: pellet densities of as-fabricated fuel lie generally around 95% of theoretical density, but may lower down to 85% (Table 1). As-fabricated pellets may be either solid pellets (ortho cylinders) or annular pellets (see Section 2.03.7.1).

For SFRs, mixed oxide fuel is hypostoichiometric: O/M ratio (where M denotes U + Pu) of as-fabricated pellets lies typically in the range 1.93–1.99.

2.03.2.3 Operating Conditions

Fuel pins of fast reactors are designed to operate at a high Linear Heat generation Rate (LHR): between ~400 and 500 W cm^{-1}, at the level of the maximum neutron flux plane, about twice higher than standard linear power in light water reactors (LWRs). As the fast reactor fuel pin diameters are generally smaller than classical rod diameters of LWRs, the power density and heat fluxes are much higher in fast reactors than in LWRs. For example, in a Phénix fuel pin at 450 W cm^{-1}, the power density in the pellet reaches almost 2000 W cm^{-3} and the heat flux in the gap between fuel and cladding is 260 W cm^{-2}, whereas in a pressurized water reactor (PWR), these values are about 400 W cm^{-3} and 80 W cm^{-2}.

Due to the low height to diameter ratio of the fast reactor cores, the axial profile of neutron flux and linear heat rate is rather peaked, with a maximum to mean ratio ($\phi_{max.}/\phi_{mean}$) in the range 1.2–1.3.

The LHR of the fuel pins, which depends on the position in the core, generally decreases continuously due to depletion of fissile materials with the burnup. The higher the initial plutonium content, the higher the decrease rate.

The sodium coolant of the primary circuit is not pressurized, but its weight induces a few bars of pressure in the bottom part of the fuel bundle. Sodium enters the bottom part of the core at about 400°C or slightly lower, and the average coolant temperature above the core is typically about 550°C. Locally, the temperatures may be higher and fuel pins for fast reactors are designed to withstand maximum cladding temperatures above 600°C (typically between ~620 and 650°C).

The neutron flux is very intense ($\sim 7 \times 10^{15}$ n cm^{-2} s^{-1} in the core center) and the population of neutrons in the core has high energy (in the range 10^5–10^6 eV). Consequently, the metallic materials in the subassembly (cladding, spacer wire, and hexagonal wrapper tube) suffer high irradiation damage, more than 100 dpa NRT (displacement per atom) at high burnup (~ 150 GWd t_{HM}^{-1}). This was one of the main challenges in the development of fast reactors: qualifying metallic materials able to withstand such high damage while keeping to a certain extent, their dimensional stability and suitable mechanical properties.

For prototype SFRs, the mean residence times of fuel subassemblies lie in the range 400–800 days and the mean length of a reactor cycle is typically around 100 days. Even if some shuffling is possible to balance core power, fuel subassemblies remain in the same zone (inner or outer core) during their whole life.

2.03.2.4 Main Objectives and Requirements of Fast Fuel Development

In order to reduce fuel cycle costs, the main objective of oxide fuels R&D for fast reactors has been to reach high burnup, typically around 150 GWd t_{HM}^{-1}, about twice the burnup achieved in LWRs. First experimental results demonstrated that the oxide fuel is able to reach very high burnups: in Rapsodie, for example, a burnup above 25 at% (~ 240 GWd t_{HM}^{-1}) had been achieved in the 1970s. The main difficulty has been to reach high burnups for oxide fuel pins irradiated in representative conditions, which means with high damage dose on the cladding, while complying with all reliability and safety requirements. **Table 1** gives some indications on the maximum burnups that have been achieved in the different prototypic reactors. Altogether, about 10,000 oxide fuel pins have reached a burnup of 15 at% (~ 144 GWd t_{HM}^{-1}).

The main requirements and design criteria are the following:

- Guaranteeing the absence or a small fraction of fuel melting, both in nominal conditions and during off-normal events (The value may depend on the Nuclear regulatory commission of each country). This criterion must be fulfilled with a high confidence level, that is, taking into account all uncertainties. It has been the main factor limiting the linear heat generation rate of fuel pins,
- Keeping cladding integrity and fuel pin tightness. The probability of cladding failure in nominal conditions must remain low ($\sim 10^{-5}$) in order to guarantee a low activity of sodium coolant. Experience showed that the main cause of failure in fast reactor oxide pins was related to excessive clad deformation because of austenitic steel swelling. This was up to now the main factor limiting the increase of in-reactor lifetime and fuel burnup. In fact, the limitation was not on burnup but on the maximum dose the cladding material could withstand. Indeed, other causes of fuel failures have also to be taken into account, in particular, loadings due to mechanical interaction between fuel and cladding, in particular, during a rise in power after a long operation at reduced power, or a significant loss of ductility or strength due either to irradiation embrittlement or a decrease in the width of sound material due to severe fuel cladding chemical interaction (FCCI),
- Cooling of the fuel pin bundle must be ensured up to high burnup in all operating conditions. Again, clad and wire deformations induced by austenitic steel swelling appeared to be the main limitation as they alter the bundle thermal-hydraulics, eventually leading to local overheating and also to mechanical interactions,
- Loading and unloading of subassemblies have to be guaranteed, which induces a limitation on the deformation of the hexagonal wrapper tubes. If it is manufactured with austenitic steel, swelling induces an increase in the flat to flat width of the wrapper tubes and also, in the periphery of the reactor core, a bowing of subassemblies due to a swelling gradient through the subassembly. In addition, the small inner pressure of sodium (a few bars) may induce deformation of the wrapper flats by irradiation creep.

Demonstration of fuel compliance to the various requirements is done with the help of fuel performance codes, which take into account all the known phenomena and which have been developed and validated against experimental results.

2.03.3 Behavior at Beginning of Life

2.03.3.1 Temperature Distribution in Oxide Pellets

Most phenomena occurring inside oxide fuel pellets are thermally activated, and a good knowledge of the thermal field inside the fuel stack is of paramount importance.

2.03.3.1.1 Thermal conductivity of oxide fuel

Thermal conductivity of oxide fuel is the key property to calculate the temperatures in the fuel pellets and it has received much attention. (U, Pu)O_2 oxide fuel is an ionocovalent material with a rather poor thermal conductivity, in the range of 2–3 W m^{-1} K^{-1} in the operating temperature range for an as-fabricated oxide 100% dense. At low temperatures, up to about 1800K heat migrates by a phonon mechanism, while at higher temperatures, electronic conductivity is predominant. The correlation used for thermal conductivity λ of oxide has generally the following form: the first term applying to phonon

conduction λ_{ph} and the second term λ_e predominant at high temperatures refer to electronic conduction with a possible contribution of heat transfer by radiation

$$\lambda = \lambda_{ph} + \lambda_e = \frac{1}{a + bT} + \frac{d}{T^2} \exp\left(-\frac{Q}{T}\right)$$

where the coefficient "a" accounts for phonon scattering by point defects of the lattice and the "bT" term stands for the contribution from the enharmonic interaction between phonons.

In addition, conductivity of the oxide decreases with the porosity p and its morphology (about 14% of decrease for a porosity of 5%). λ also decreases sharply as the O/M ratio deviates from 2.00. As oxide fuels used in fast reactors are slightly hypo stoichiometric, (typically with a O/M ratio after fabrication near to $\sim$1.97) this deviation from stoichiometric compositions leads to a further decrease in conductivity at the beginning of life.

Last but not the least, thermal conductivity decreases during irradiation as a consequence of the growing presence of various compounds of fission products and irradiation-induced point defects. Nevertheless, this last effect is partly compensated by an increase in O/M ratio resulting from fission.

2.03.3.1.2 Temperatures inside the fuel pin

The heat produced inside the fuel pellet flows toward the coolant through the gas gap and the cladding. As the external cladding temperature T_{ec} is known, the inner temperature T_{ic} is deduced from the heat equation in the cladding:

$$T_{ic} - T_{ec} = \frac{P_l}{2\pi\lambda_c} Ln\left(\frac{r_{ec}}{r_{ic}}\right)$$

where P_l is the Linear Heat Rate, λ_c is the thermal conductivity of the cladding, and r_{ec} and r_{ic} are the external and the internal cladding radii.

The heat flux flowing through the gas gap between the fuel and the cladding is proportional to the difference between the surface temperature T_s of the fuel pellet and the cladding inner temperature T_{ic}:

$$T_s - T_{ic} = \frac{1}{h}\frac{P_l}{2\pi r}$$

where r is the pellet radius. The heat transfer coefficient h is the sum of three terms:

$$h = h_c + h_R + h_{cond}$$

- h_{cond}: conductive heat transfer coefficient is linked to the width of the gap and to the gas conductivity. This is why the pins are filled with helium that is the inert gas with the highest thermal conductivity. The heat transfer from fuel to gas and from gas to cladding introduces an additional resistance term that needs to be taken into account. As long as the fuel/cladding gap is open, conduction plays a predominant role.
- h_R: radiative heat transfer coefficient. As a T^4 term intervenes in this coefficient, the contribution of radiation to heat transfer is generally very low in nominal irradiation conditions.
- h_c: contact or solid-solid heat transfer coefficient, different from 0 when the gap is closed, is linked to contact pressure and to roughness of the fuel and cladding surface.

Inside the fuel pellet, the radial flux depression can be disregarded in fast reactors. In the case of a solid pellet, the heat equation may be simply written:

$$\int_{T_s}^{T_c} \lambda dT = \frac{P_l}{4\pi}$$

where T_c and T_s are the center and the surface temperatures of the fuel pellet, and λ is the fuel thermal conductivity.

Examples of typical radial temperature profiles are given in Fig. 1 for a linear power of 450 W cm^{-1}. Center temperature may exceed 2000°C, with a thermal gradient reaching several thousands of kelvins per centimeter. These very high operating temperatures, much higher than in oxide fuel irradiated in thermal reactors, will induce several phenomena specific of oxide behavior in fast spectrum and considerable changes of microstructure during the initial irradiation period.

2.03.3.2 Fuel Restructuring

2.03.3.2.1 Pellet cracking

The radial temperature gradient in the fuel induces internal stresses since the center tends to expand more than the periphery. In a plane strain approximation, the hoop and axial stresses σ_θ and σ_z at the surface of the pellet are tensile stresses given by:

$$\sigma_\theta = \sigma_z = \frac{E\alpha}{2(1-\nu)}(T_c - T_s)$$

With:

- E: Young's modulus ($\sim$168 GPa at 1000°C),
- α: thermal expansion coefficient ($\sim 10.10^{-6}$K^{-1}),
- ν: Poisson's ratio ($\sim$0.31).

At low temperature, under about 1400°C, oxide is brittle, with a rupture stress of about 130 MPa. A 100°C difference between T_c and T_s is sufficient to induce tensile stresses at the periphery of the pellet of about 120 MPa, which means that oxide fuel pellets start to crack at the very beginning of the first power rise when LHR is still 10% of full power. Pellet cracking is the first phenomenon occurring in the oxide fuel pellet at beginning of life. At the end of power rise, the central area of oxide pellets becomes ductile, but many radial and axial cracks have already been formed.

2.03.3.2.2 Formation of columnar grains and central hole

Because of the very high temperatures and steep temperature gradients, spectacular changes in the microstructure occur in a short time, during the first hours and days at full power. Fig. 2 gives an example of this restructuring effect.

In the central area of the pellets, that is, at very high temperatures (≥2000°C), pores take a disk shape, a few micrometers thick (~5–10 μm) with a diameter of several tens of micrometers (~50–100 μm), the axis of symmetry oriented in the thermal gradient: they are called: 'lenticular pores'. Between the hot and the cold faces of these lenticular pores, the thermal gradient $(dT/dx)_p$ is greater than the gradient $(dT/dx)_f$ in the neighboring fuel:

$$\left(\frac{dT}{dx}\right)_p = \frac{\lambda_f}{\lambda_p}\left(\frac{dT}{dx}\right)_f$$

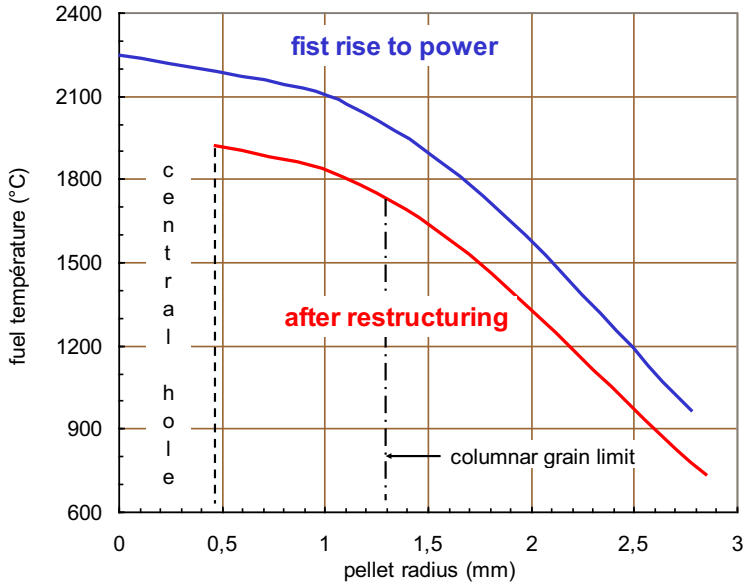

Fig. 1 Radial temperature profile in oxide pellet calculated in a Phénix pin at first rise to power and after restructuring and central hole formation.

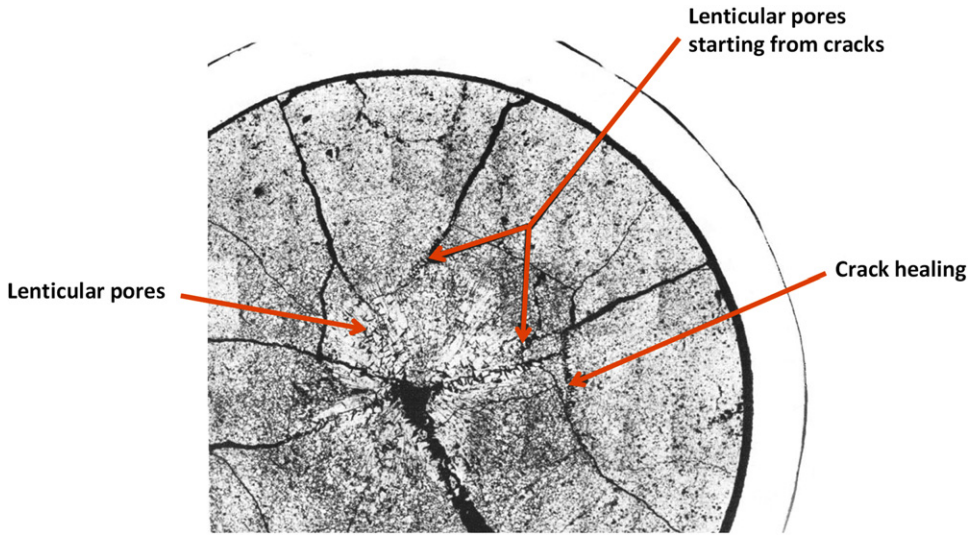

Fig. 2 Micrograph of an oxide pellet irradiated at start-up of Rapsodie during 4 h at 380 W cm^{-1}.

λ_f/λ_p, the ratio of fuel thermal conductivity to the conductivity of gas contained in the pores is much higher than 1. The gas contained in these pores is a mixture of helium that has been filled in the pin during the fabrication, with small amounts of fission gases (xenon and krypton) and spurious gases (essentially CO) arising from impurities.

The pressure of the fuel vapor in equilibrium with the oxide is higher on the hot side of the lenticular pore than on its cold side. This difference in vapor pressures induces an evaporation–condensation mechanism: matter evaporating from the hot face and condensing on the cold face travels down the thermal gradient, inducing an inverse displacement of the lenticular pores that climb the thermal gradient toward the center of the pellet.

The displacement velocity of the pore v_p is an increasing function of the temperature gradient $(dT/dx)_p$, the oxide vapor pressure (and therefore the temperature), and the diffusion rate D_g of the oxide molecules through the gas contained in the pores. D_g decreases with the pressure in the pores (a few atmospheres) and the atomic mass of the gas:

$$v_p = A\frac{D_g}{T^3}\exp\left(-\frac{\Delta H_v}{kT}\right)\left(\frac{dT}{dx}\right)_p$$

where ΔH_v is the vaporization enthalpy.

The oxide vapor condenses on the cold side in a nearly single crystal way. While moving toward the pellet center, the lenticular pores destroy the initial fuel microstructure and leave behind them a dense fuel ($\sim$97% TD) in very elongated crystal grains (up to 1 mm long by a few tens of micrometer width) called 'columnar grains' that appear clearly in micrographs (see Fig. 2). The grain boundaries of these columnar grains are delineated by trails of small spherical pores ($\sim$1 μm) that have been left from the periphery of the large lenticular pores during their migration.

The emergence of these lenticular pores at the center of the pellet leads to the formation of a central hole in as-fabricated full pellets. The cracks' volume of the central area and a fraction of the pellet initial porosity and of the initial gap are thus transferred toward the central hole. During the first stage of the process, cracks are the main source giving rise to lenticular pores, and migration of these pores is the main mechanism for healing the cracks.

At very high temperatures ($\geq$2000°C), this migration of lenticular pores by vapor transport is a very efficient mechanism to form columnar grains and central void: a large part of this fuel-restructuring process has taken place in a few hours. At lower temperatures in the range 1800–2000°C, even if lenticular pores are not systematically observed, elongated grains may be formed resulting from grain growth and migration in the thermal gradient of spherical pores. This migration can occur either by vapor transport (as lenticular pores) or by volume diffusion in the oxide surrounding the pore.

The displacement velocity of the pores varies very rapidly with temperature, and the columnar grains only form at high temperatures above $\sim$1800°C. This external limit of the columnar grains, that is, the frontier between columnar grains and equiaxed grains, is often used to deduce thermometric information, assuming that the observed microstructural changes can be correlated to a fixed temperature. This assumption is not fully rigorous, as not only temperature but also temperature gradient and time play a role in these restructuring mechanisms, and the temperature at a given radius is continuously evolving as a consequence of gap closure and restructuring effects. Nevertheless, this assumption gives an approximation and helps in validating the thermal calculations of the fuel performance codes: the higher the temperature, the greater the diameters of the central hole and of the columnar grains.

In the case of annular pellets, these restructuring mechanisms occur in a similar way, inducing a diameter increase of the initial central hole at all levels with high linear heat rates ($\geq$350 W cm^{-1}). These mechanisms are also efficient in the case of vibrocompacted fuel: the vibropacked microstructure disappears from the central area, and a central hole and columnar grains appear quite similar to those observed in full pellets.[8]

One of the main consequences of this restructuring is a decrease in the center temperature resulting from two effects that add up: the geometry change, especially when a full pellet is transformed into an annular pellet, and the slight decrease of porosity with a positive effect on fuel thermal conductivity.

2.03.3.2.3 Grain growth

Micrographs of the irradiated oxide fuel reveal an increase in grain size in a ring outside the columnar grain region, for temperatures of about 1300–1800°C. This grain growth results from the displacement of grain boundaries induced by a reduction of the energy linked to surface tension of the boundaries; smaller grains disappear to the benefit of larger ones.

This grain growth mechanism, which also occurs during out-of-pile annealing of the oxide pellets, has a faster kinetic in reactor, at least at low burnup, because of irradiation-enhanced diffusion. However, at high burnup, grain boundaries are blocked by an accumulation of intergranular gas bubbles and fission product precipitates.

2.03.3.2.4 Summary

The main morphological consequences of the high thermal regime in a SFR oxide fuel pin: pellet cracking, grain growth and formation of columnar grains and a central hole are highlighted Fig. 3:

2.03.3.3 Redistribution of Fuel Constituents

Because of the high temperatures and of the very large temperature gradients, radial redistributions of constituents have been systematically observed. These redistributions are made possible by vapor transport, thanks to radial cracks and interconnected

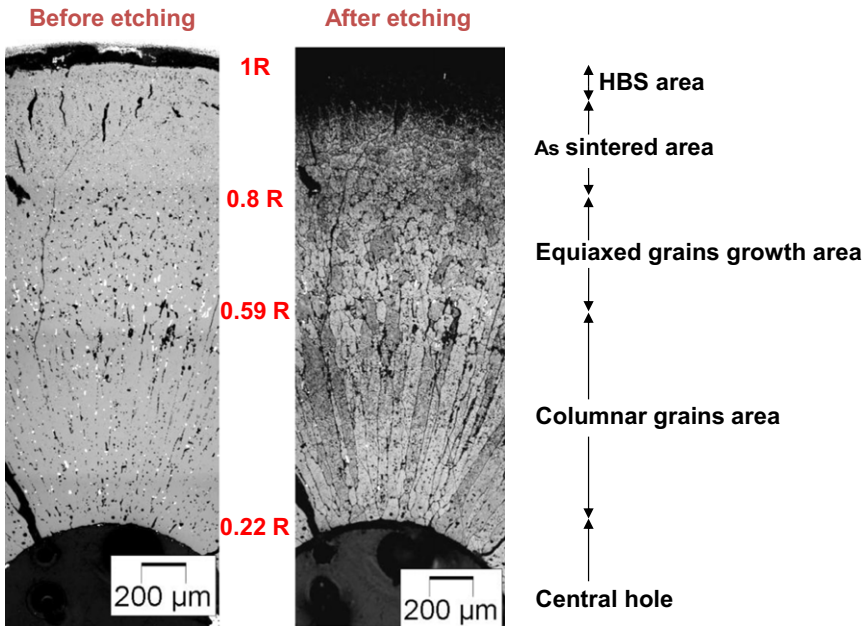

Fig. 3 Radial cross-section of a Phénix fuel Pin with a plutonium content of 22% irradiated at 400 W cm^{-1} and 13 at%.

porosity, which provide easy paths for transport, allowing communication between the hot and the cold areas of the fuel pellets. Migration of components also occurs in the solid phase by thermal diffusion; the driving forces for radial migration obey the laws of irreversible thermodynamics.

2.03.3.3.1 Oxygen redistribution

The as-fabricated oxide pellets to be used as fuel in fast reactors are always hypostoichiometric with an initial O/M ratio typically in the range 1.93 to <2.00. Some experiments have shown that in the early stages of irradiation, oxygen is redistributed radially, migrating down the thermal gradient, thus bringing the composition close to stoichiometry near the periphery, whereas the O/M ratio becomes lower than the fabricated value in the hottest area. This oxygen redistribution occurs without affecting the mean O/M ratio of the pellets. Most of these experiments have been performed in out-of-pile tests, but a few results were obtained from in-pile experiments. **Fig. 4**, for example [9], shows the local O/M values as a function of pellet radius for different initial O/M ratios. These local O/M ratios were deduced from lattice parameters measured on the oxide powder taken out of concentric rings micro-drilled in irradiated pellets. These pellets were extracted from fuel rods with different initial O/M ratio irradiated in thermal reactor to very low burnup, then quenched at the end of irradiation in order to avoid any oxygen redistribution during cooling.

Because of the high oxygen diffusion rate, this radial redistribution of oxygen occurs very rapidly during the first power rise, as it may be concluded from the experiments on pins equipped with a thermocouple in the central hole.

Studies of this phenomenon have been carried out mainly in the 1960s and 1970s. Several mechanisms have been proposed to explain this redistribution.

2.03.3.3.1.1 Oxygen migration by vapor transport

One of the first proposed models is based on the assumption that oxygen is transported in a gaseous mixture of CO and CO_2[10,11] (it could be also a mixture of H_2 and H_2O). The carbon is provided by the fuel, as there is always some parts per million of carbon as an impurity in the oxide and may volatilize as CO or CO_2 at operating temperatures. The model assumes that radial cracks and interconnected porosity provide pathways for vapor transport: as a result, the partial pressures of CO and of CO_2 are constant over the pellet radius, and the ratio CO/CO_2 is constant in the pellet despite the temperature gradient. Thermodynamic considerations require that all along the radius, oxygen pressure corresponding to the ratio P_{CO}/P_{CO2} is in equilibrium with the local oxygen potential $\Delta G(O_2)$ of the fuel. As $\Delta G(O_2)$ is a function of T and O/M ratio, such an equilibrium implies that the O/M ratio varies along the radius as a result of oxygen migrating down the thermal gradient.

Such a model allows predicting an oxygen redistribution profile in reasonable agreement with the experiments. This mechanism of vapor transport certainly exists, but it alone cannot explain the oxygen redistribution.

- At low temperatures in the periphery of the pellets (~1000°C), the partial pressure of CO_2 in equilibrium with the fuel is very low ($\sim 10^{-3}$ Pa) and the transport mechanism would require a very long time, while experiments have shown it is a very fast phenomenon,
- Thermal diffusion of oxygen in the solid is rapid and the chemical driving forces due to a no uniform distribution would induce oxygen migration that would strongly reduce the extent of oxygen redistribution.

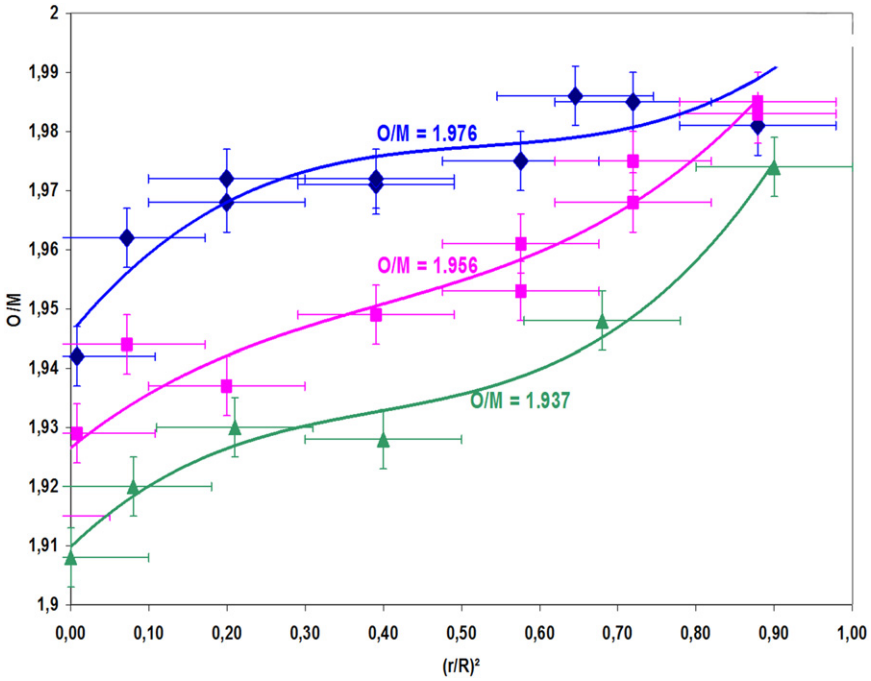

Fig. 4 O/M radial profiles measured in irradiated $(U,Pu)O_2$ fuel for various initial O/M ratios.

2.03.3.3.1.2 Oxygen migration in solid phase

These models[12–14] are based upon the theory of irreversible thermodynamics and on the observation in laboratory experiments that oxygen redistribution can occur even in fully dense mixed oxide with no pathways for gas transport. By thermal diffusion, oxygen vacancies climb the thermal gradient and accumulate in the hot central region inducing a decrease of the O/M ratio in this area. Chemical diffusion of oxygen counterbalances this effect and a balance is rapidly found corresponding to the radial oxygen redistribution profile.

Several equations and models have been proposed to calculate this oxygen redistribution. One of the simple ones is the following[12]: in a thermal gradient, the value of x in $(U,Pu)O_{2-x}$ should vary locally with the temperature T according to:

$$\ln x = \frac{Q^*}{RT} + K$$

Q*, the characteristic heat of transport, is determined empirically; for slightly hypo stoichiometric oxide, the proposed values for Q* are about −125 kJ mol^{-1}; for other O/M values, Q* is a function of the deviation from stoichiometry and of the plutonium content.

This radial oxygen redistribution in the pellets has several consequences:

- The center temperature decreases slightly, as the increase in the O/M ratio in the periphery improves the fuel thermal conductivity in the region that experiences the highest thermal flux,
- The oxygen potential at the pellet surface also increases slightly, with potentially adverse effects on the corrosion of the cladding,
- Diffusion coefficients of many species depend upon the O/M ratio and will be affected by oxygen redistribution,
- In case of clad failure, the extent of reaction between the fuel and sodium will be enhanced, as this reaction occurs with fuels with a high O/M ratio and requires a source of oxygen.

2.03.3.3.2 Plutonium redistribution

Microprobe examinations performed on irradiated oxide pellets generally exhibit plutonium enrichment in the central area near the central hole, and slight plutonium depletion in a ring located near the periphery of columnar grains. Contrary to oxygen redistribution, the plutonium redistribution does not affect the whole radius but only the central hot region (T ≥1800°C), a consequence of much slower actinide diffusion as compared to oxygen diffusion. **Fig. 5** gives an example of such plutonium redistribution measured at high burnup, but a major part of this redistribution had occurred at the beginning of life. Plutonium content varies from about 20% at the periphery of columnar grains up to about 30% near the central hole.

This plutonium redistribution starts at the very beginning of irradiation: Electron probe microanalysis (EPMA) measurements have been performed in 2009 on oxide pins that had been irradiated only 10 min and 24 h at full power (430 W cm^{-1}) and a significant plutonium redistribution could already be observed.[15]

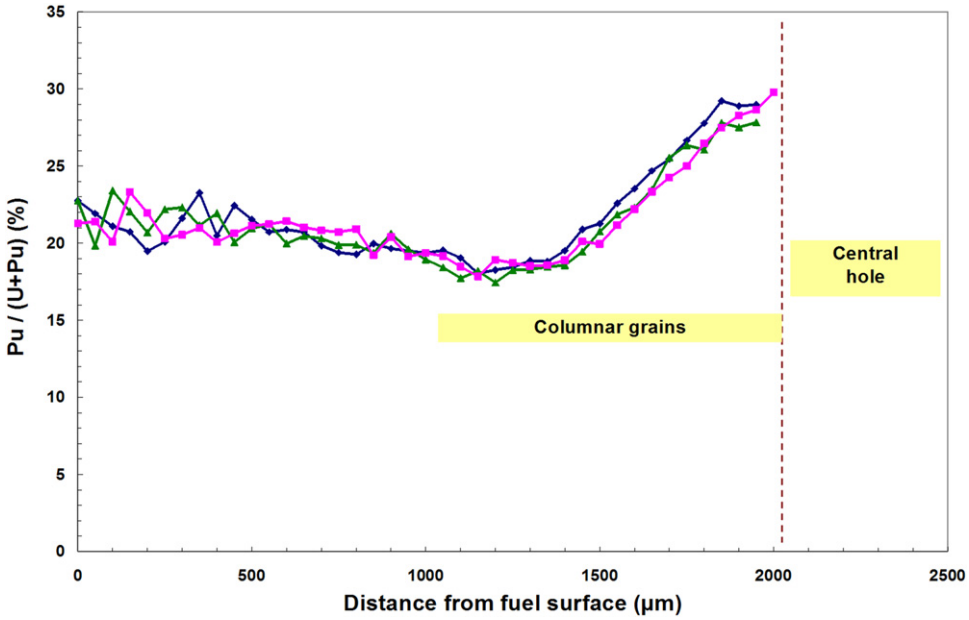

Fig. 5 Plutonium radial profile measured by electron probe micro analysis on mixed oxide pellet irradiated in Phénix at 15 at%.

As for the oxygen redistribution, several mechanisms and models have been put forward to explain such actinide migration under thermal gradient, the key processes being again vapor transport and solid diffusion.[13,16,17]

The increase in the plutonium content in the central area of the fuel lowers the melting temperature of the MOX and may possibly increase the dissolution time of the spent fuel during the reprocessing.

2.03.3.3.2.1 Plutonium redistribution by vapor transport

An obvious mechanism of plutonium redistribution is directly linked to the mechanisms of fuel restructuring and especially the evaporation–condensation phenomenon. The evaporation is not congruent: above slightly hypo stoichiometric oxide (for O/M ratio in the range $\sim$1.95–2.00), the partial pressure of UO_3 is much higher than the other actinide oxide species. The actinide oxide vapor in equilibrium with the solid is, therefore, enriched in uranium, and in a radial temperature gradient, UO_3 will preferentially evaporate from the hot zone, resulting in plutonium enrichment in the hot area and condense in colder area where the vapor pressure becomes too low to have significant effects.

The radial migration of lenticular pores by evaporation–condensation is one of the mechanisms responsible for this plutonium redistribution, nevertheless with a limitation on its efficiency. As soon as the lenticular pore starts to migrate up the temperature gradient, the hot side of the pore is highly enriched in Pu while the cold side is depleted.[18] As the pore velocity is much higher than the plutonium diffusion rate, the narrow zone with an excess plutonium on the hot side is pushed forward of the migrating pore and the evaporation of the hot side of the pore is an oxide whose plutonium content is much higher than that of the pore average value.

Vapor transport may also occur, thanks to the radial cracks and open porosity as long as these pathways remain open.

For very low O/M ratios ($\leq$1.94), PuO becomes the actinide oxide species with the highest partial pressure. Consequently, the plutonium redistribution is reversed and plutonium depletion can be observed near the central hole of highly hypo stoichiometric oxides, but this occurs for O/M ratios at the limit of the O/M range generally considered to be used in commercial fast reactors.

2.03.3.3.2.2 Plutonium redistribution by solid diffusion

As for oxygen redistribution, according to irreversible thermodynamics, a temperature gradient applied to a mixed oxide will induce a flux of atoms. The causes of thermal diffusion are the differences of the lattice energies of the fuel components in the temperature gradient. Migration of plutonium can be described using again Q* the heat of transport of plutonium in the solid. The flux J_{Pu} of plutonium atoms is given by the equation:

$$J_{pu} = -D\left[\frac{\partial c}{\partial r} + c(1-c)\left(\frac{Q^*}{RT^2}\right)\left(\frac{\partial T}{\partial r}\right)\right]$$

where D is the diffusion coefficient of plutonium and c is its volumetric concentration. Q* is determined empirically from plutonium redistribution measured on irradiated fuel pellets or in laboratory experiments. A large range of values (from −35 to −240 kJ mol^{-1}) have been published in the literature, the negative sign indicates that plutonium migrates up the thermal gradient.

The main consequence of this plutonium redistribution is a small decrease in the margin to fuel melting for two reasons. The first small effect related to the Pu-enriched area near the central hole is a slight increase in the power generation at a place more distant from the coolant, which slightly increases the center temperature. The second and more significant consequence is a

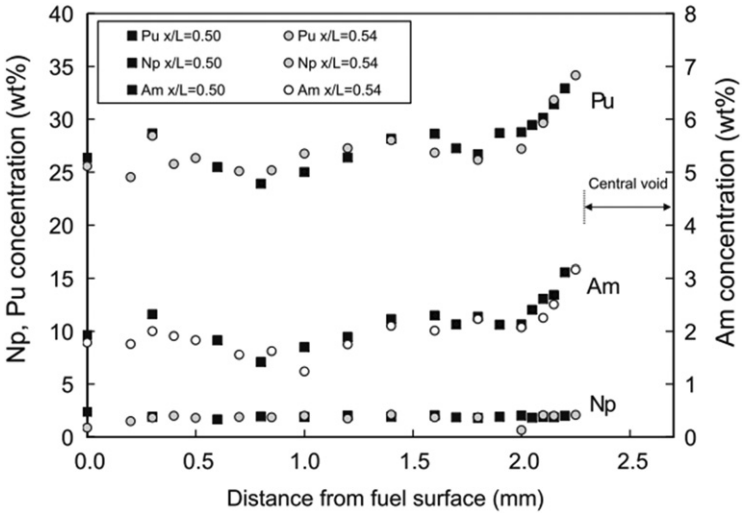

Fig. 6 Radial profiles of Pu, Np and Am in a $(U_{0.672}\ Pu_{0.288}\ Am_{0.02}\ Np_{0.02})O_{1.98}$ irradiated 24 h at 432 W cm^{-1}. Reproduced from Maeda, K., Sasaki, S., Kato, M., Kihara, Y., 2009. J. Nucl. Mater. 385, 413–418.

decrease in the fuel melting temperature due to the increase in Pu/M: for example, when plutonium content rises from 20% to 30%, solidus temperature decreases by about 30°C.

2.03.3.3.3 Redistribution of minor actinides

In Generation IV systems, recycling of minor actinides (MA) (i.e., mainly americium and neptunium, and possibly curium) is envisaged in order to decrease the amount of long-lived radionuclides going to waste. It is even a prerequisite in many countries. This could be done either in a homogeneous way, diluting a few percentages of MA in the driver fuel or in a heterogeneous way, dedicating for this recycling specific subassemblies to be irradiated either in the core or in the radial blanket.[19]

In case of homogeneous recycling, the question arises as to how a few percentages of Am or Np will behave at beginning of life and how redistribution processes will affect them. Recently, the Japanese experiment "Am1" provided answers to this question.[15,20] Several MOX fuel pins, with about 30% Pu, two O/M ratios (1.98 and 1.95), and various contents of MA (2% Am + 2% Np or several americium contents up to 5%) were irradiated in the experimental reactor Joyo at a LHR of 430 W cm^{-1} during short times (either 10 min or 24 h). Fig. 6 shows an example of the results as measured by EPMA: americium redistributes as plutonium with a strong enrichment in the hot area (Americium content rises from 2% to 3% near the central hole), while neptunium profiles exhibit no radial redistribution. The authors explain these results by vapor transport: for slightly hypo stoichiometric oxides, the UO_3 vapor pressure is higher than the vapor pressures of both Pu- and Am-bearing gas species. However, these gas pressures are still known with rather high uncertainties, and the radial stability of neptunium is not yet explained; studies in this field are under progress.

2.03.3.4 Geometrical Evolution

2.03.3.4.1 Gap closure

Although the thermal expansion coefficient is lower in oxide fuel than in austenitic stainless steel cladding (typically about 10×10^{-6} in oxide vsersus 17×10^{-6} in steel), the temperatures in the fuel pellets are much higher than in the cladding and induce a higher thermal expansion in the fuel pellets. The gap size under hot conditions is therefore smaller than as-fabricated gap size: for example, in a standard Phénix fuel pin, the diametrical gap size under hot conditions becomes about 150 μm for an initial value of 230 μm independently from the central hole formation or fuel fragment relocation.

Post irradiation observations of fast reactor pins irradiated with a sufficient LHR and at low burnup show that the fuel clad gap, as observed at room temperature, decreases rapidly until it is completely closed. At high LHR (≥400 W cm^{-1}), gap closure is completed after a burnup of about 1 at% or even less, while at lower linear powers, in particular, close to the bottom and top of fuel columns, gap closure needs more time (several atomic percentage). This gap closure results from several mechanisms: relocation of pellet fragments and axial creep of the fuel stack intervene in a very short time (a few hours), while the effects of fuel gaseous and solid swellings need longer time and some burnup to accumulate.

- Fuel pellets are broken into several fragments at the end of first rise to power. Due to vibration in the pins, each fragment can move with respect to the others in a stochastic manner, resulting in a small average displacement of matter toward the cladding. This mechanism called 'fuel relocation' is probably responsible for a significant fraction (~20%) of the gap closure. As the cracks are healed in the central area, this mechanism can occur each time the reactor is shut down, but with smaller extent than the first time,

- Under the effect of the force exerted on the fuel column by the spring located in the upper part of the pin, plus the own weight of the fuel stack, an axial compression creep occurs in the oxide especially near the peak power node (see Section 2.03.3.4.2). Consequently, this induces an additional diameter expansion of fuel pellets ($<10\%$), which slightly contributes to gap closure,
- However, the main cause of gap closure is probably the swelling of the fuel including a part of gaseous swelling. At high temperatures ($\geq$1300°C), the precipitation of spurious gas due to carbon impurities can contribute to gaseous swelling at the very beginning of life. In addition, fission gas bubbles can grow and coalesce and also generate large rates of gaseous swelling.

However, this large swelling rate can hardly be measured because it is a dynamic swelling: in the hot central area, these gas bubbles rapidly migrate toward the central hole, gas is released, and the unique observable consequence of this gas swelling and sweeping is an overall displacement of the oxide from the center toward the periphery.

With a large gap, the difference of temperature between the outer pellet and the inner cladding may reach several hundreds of degrees centigrade; therefore, this gap closure induces a large decrease in fuel temperatures (see Fig. 1).

2.03.3.4.2 Evolution of fuel stack length

At the first rise to full power, due to thermal expansion, both lengths of fuel column and pin cladding increase. As the temperatures are much higher in the oxide fuel than in the cladding steel, the axial expansion is higher in the fuel column than in the cladding. For rapid rise to power, as it has been seen, thanks to the hodoscope (The hodoscope in the Cabri safety test reactor is a neutron radiograph device allowing instantaneous scan of the whole length of the fuel column; it allows to follow fuel movements in real time) in some Cabri experiments, the fuel length can increase by about 2% (fuel hottest regions pilot axial expansion), while clad increase does not exceed 1%. However, at the beginning of irradiation, as a result of the load of the spring at the top of the fuel column and also due to proper weight of the fuel stack, the hottest area of the fuel creeps, and the fuel stack length decreases by several millimeters ($<0.5\%$). In addition, gap closure induces a decrease in fuel temperatures and therefore an additional decrease in fuel length.

At the time of gap closure for initially dense fuels, the increase in fuel column length is generally a few millimeters higher than the increase in cladding length. After gap closure, fuel is mechanically and chemically anchored on the cladding. Measurements of lengths at various burnup show that fuel length evolution does not depend on burnup, but is directly related to clad length evolution which is itself induced by steel swelling. In case of large clad swelling (e.g., with non-stabilized austenitic 316 grades), clad elongation stretches the fuel column, opening interpellets at the level of highest clad swelling. In case of low clad swelling (e.g., with stabilized austenitic grades or ferritic/martensitic steels), fuel elongation remains quite low; fuel is squeezed in the cladding and is generally too soft to be able to induce significant loadings and axial deformation in the cladding.

2.03.4 Consequences of Fission

For economic reasons, the main objective of oxide fuels in fast reactors is to achieve very high burnup; the reference target for burnup is typically of 15 at% or even higher. Fission of actinide atom gives birth to two new atoms, the fission products (FP), which means that, at the end of irradiation, 15% of the initial actinide atoms have disappeared and 30% new atoms are now present in the fuel pin.

Such a large change obviously induces considerable consequences on the overall behavior of the fuel pin. All physical and chemical properties of oxide fuel will continuously evolve during its lifetime in the reactor; in particular, fission products will induce a decrease of thermal conductivity as well as a decrease of melting point, thus possibly reducing the margin to fuel melting. Most phenomena occurring in the fuel pins will be a direct consequence of these fission products. This is the case for solid and gaseous swelling, resulting in fuel cladding mechanical interaction (FCMI) as well as fission gas release inducing an increase of the gas pressure inside the pins. This is also true for all the types of corrosion and the so-called FCCI where in fact oxide fuel alone could not have any harmful effect. During reprocessing, the chemical state of the fission product also influences the residues from the dissolution of spent fuel in nitric acid.

This large amount of fission products is one of the specificities of fast oxide fuel, along with the fact that high temperature and steep temperature gradient induce not only radial but also axial migration of certain categories of these fission products. All these effects depend upon the chemical state of the fission product, which is influenced by the oxygen potential of the fuel. In turn, it determines the fate of almost two oxygen atoms that are freed each fission, thus controlling the evolution during irradiation of the oxygen potential inside the fuel pins.

2.03.4.1 Formation of Fission Products and Minor Actinides

In fast oxide fuel, as in all types of fuels, the fission of plutonium creates two fission products: a light fission product and a heavy fission product. Statistically, the mass numbers of created nuclides are distributed on the classical two maxima curve. With fission of ^{239}Pu, the position of the first maximum (the light fission product) is slightly shifted toward heavier atoms as compared to fission of ^{235}U.

Most newly created atoms are very unstable and generally short-lived radionuclides. From the fuel performance point of view, we consider essentially the nuclides with rather long half-lives ($\geq$1 day) and the total quantity of a chemical element, which can gather several radioisotopes. For example, cesium that plays an important role in fuel behavior comes from three main nuclides:

^{133}Cs, ^{135}Cs, and ^{137}Cs. ^{137}Cs is mainly a decay product of the very short-lived ^{137}Xe (3.9 min), while the nearest precursor of ^{133}Cs is ^{133}Xe with a longer half-life (5.3 days). In the hot central area of the fuel pellets, this ^{133}Xe has time to partially escape the fuel before decaying into ^{133}Cs. Consequently, γ-spectrometric observations often show at the extremities of fuel column peaks of ^{134}Cs that are not perfectly associated with corresponding peaks of ^{137}Cs. This ^{134}Cs is in fact a neutron activation product of ^{133}Cs that was formed in fuel cracks and recombined with other FPs to form gaseous compounds which condensed on the nearest oxide cold spot (ends of either fissile or fertile stacks).

Table 2 gives an example of elemental yields of the main fission products. They are the average values calculated with the Darwin code system for an oxide fuel $(U,Pu)O_2$ (Initial Pu content: 23% and ^{239}Pu/Pu: 70%) irradiated up to 10 at% in inner core of Phénix.

The exact values are slightly dependent on initial isotopic composition, burnup, and neutron flux spectrum. They are gathered into several categories according to their physical and chemical states inside the fuel pellet. **Fig. 7** shows how they are distributed in the Mendeleev table.[21]

In addition to fission products, another type of new atoms is generated during irradiation in a reactor by the transmutation of actinide nuclides that capture a neutron and create a new atom with higher atomic number, essentially, neptunium, americium, and curium, called minor actinides (MA), as they are at low contents when compared to the major actinides uranium and plutonium. This mechanism, which is very efficient in thermal flux, does not introduce great changes in fast flux as the fission cross-section is much higher than the capture cross-section. In the example of the Phénix fuel, which has been used for the calculation of the fission product yields (**Table 2**), the increase of MA between 0 and 10 at% is:

- Neptunium: 0 ⇒ 0.04% of the Initial Heavy Metals (HMi),
- Americium: 0.10% ⇒ 0.16% HMi,
- Curium: 0 ⇒ 0.02% HMi.

This evolution of MA contents, especially the small production of curium, has an influence on the fuel cycle, but the consequences on in-pile fuel performance are minor and generally discarded.

Table 2 Elemental yields of fission products in a Phénix fuel pin at 10 at%

	Element	*Yield (% FP/fission)*	*Total (%/fission)*
FPs in solid solution	Y	1.9	45
	La	5.6	
	Ce	11.4	
	Pr	4.8	
	Nd	15.5	
	Pm	1.2	
	Sm	3.4	
	Eu	0.6	
	Gd	0.4	
FPs forming oxide precipitates	Rb	1.5	52
	Cs	20.1	
	Sr	3.6	
	Ba	6.8	
	Zr	19.2	
	Nb	0.2	
FPs forming metallic precipitates	Mo	21.3	75
	Tc	5.5	
	Ru	22.0	
	Rh	5.8	
	Pd	13.8	
	Ag	1.3	
	Cd	1.0	
	In	0.1	
	Sn	0.5	
	Sb	0.2	
	Te	3.5	
Gases and volatile FPs	He[a]	0.8	28
	Kr	1.8	
	Xe	23.6	
	Br	0.1	
	I	1.7	

[a]Helium is produced by ternary fissions (~0.2% of fissions), alpha decay of some actinide isotopes (especially ^{242}Cm) and reaction with oxygen ($^{16}O + {}^{1}n \rightarrow {}^{13}C + {}^{4}He$) of neutrons high energy (>2.3 MeV).

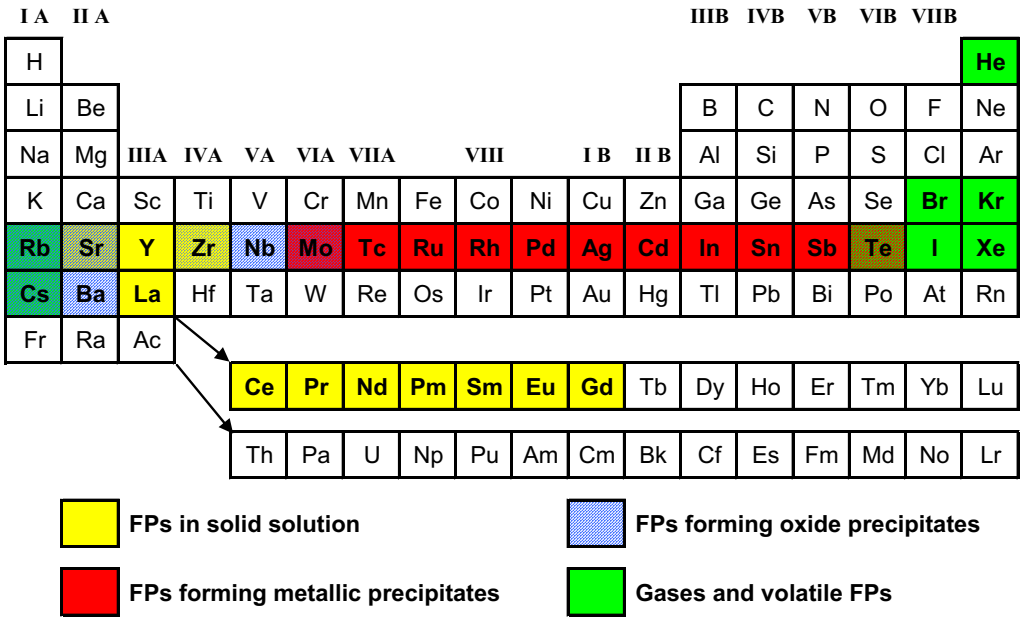

Fig. 7 Distribution of main fission products in the periodic table.

2.03.4.2 Chemistry of Fission Products

The role the fission products play on the behavior of the fuel pins depends directly upon their physical and chemical state, which depends on the local values of temperature and oxygen potential and on the thermodynamics properties of fission product species.[20]

2.03.4.2.1 Fission products in solid solution

Yttrium and all the rare earth (RE) fission products (La, Ce, Pr, Nd, Pm, Sm, Eu) are largely miscible in the oxide matrix. The RE atoms occupy an actinide site in the crystal lattice, and therefore can hardly migrate; in post irradiation examination of safety test, their axial distribution, as observed by γ-scanning (e.g., on ^{140}La or ^{154}Eu), gives good information on the axial movements of oxide fuel. A large fraction of zirconium and a smaller fraction of strontium and niobium are also dissolved in the fuel oxide; the remaining part of these fission product forms precipitated oxides. Some other fission products (such as Ba, Cs, or Te) are slightly miscible with mixed oxide, but only in small quantities.

These fission products in solid solution induce a decrease of the oxide thermal conductivity and a slight decrease of the lattice parameter. They also have an influence on the chemical properties of the fuel; for most of RE oxides, the valence in the oxide phase is 3, while the valence of the U or Pu atoms is 4. This results in a trend to increase the oxygen potential with the burnup even at a constant O/M ratio (in irradiated fuels, M stands for U + Pu + FPs in solution).

2.03.4.2.2 Fission products forming oxide precipitates

From a thermodynamics point of view, barium and zirconium must be in an oxidized form, but barium has a limited solubility in the phase $(U,Pu)O_2$ because of the large ionic radius of Ba^{2+}. These FPs precipitate therefore in the form of a perovskite structure phase $BaZrO_3$ that appears on optical micrographs at high burnup as gray inclusions. Other fission products may be partly dissolved into this perovskite phase: Sr and Cs may substitute with Ba; U, Pu, Mo, and some RE (especially cerium that is a decay product of ^{140}Ba) may occupy the Zr site of the perovskite lattice. The oxide precipitates are finally compounds of the type $(Ba,Sr,Cs)(Zr,U,Pu,Mo,RE)O_3$.

2.03.4.2.3 Fission products forming metallic precipitates

On the micrographs of fuel irradiated at high burnup, white inclusions are systematically observed (Fig. 8), the higher the burnup and the temperature, the larger these precipitates.

They are generally several micrometers in size, up to 20 μm in the columnar grain region. In some cases, in pins that have experienced high central temperatures, large particles ($\sim$1 mm) of metallic precipitates may form in the central hole, demonstrating the capacity of these metallic elements to migrate radially and even axially. The presence of such ingots can be detected on γ-scanning, especially on the ruthenium (^{103}Ru and ^{106}Ru).

In most cases, EPMA on these precipitates shows essentially five elements: Mo, Ru, Tc, Rh, and Pd. They are the five 'noble metal' fission products with the highest yield (see Table 2). This five-metal phase crystallizes in a hexagonal structure and melts slightly below 2000°C, which means that in reactors, these precipitates can be liquid in the hot central area, explaining how large ingots may form in the central hole. For Ru, Tc, and Rh, most of the production is probably located in these metallic precipitates. It is not the case

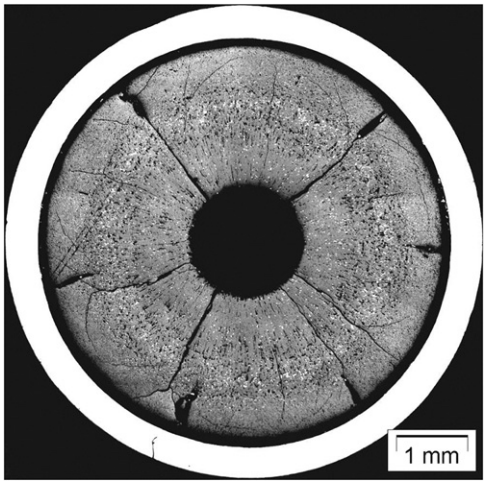

Fig. 8 Metallography of an oxide fuel irradiated in Phénix at 13 at% showing central hole (initially solid pellets), columnar grains, white metallic precipitates in and at periphery of columnar grains and a JOG (not visible) between fuel and cladding.

for molybdenum: depending upon the burnup and the initial O/M ratio, the main part of produced Mo may be found either in the metallic precipitates or in oxidized phases as a result of the evolution of oxygen potential (see Section 2.03.4.3).

At high burnups, in addition to these classical 'noble metal' precipitates, another type of metallic precipitates is observed with a different composition: EPMA reveals essentially the presence of palladium and tellurium with traces of tin, antimony, and sometimes plutonium. These precipitates, predominantly found on the periphery between the fuel surface and the cladding, result from the high vapor pressure of palladium but they can also be found in hotter parts of the fuel.

2.03.4.2.4 Volatile fission products

Volatile fission products are the fission products that are in solid or liquid phase at temperatures at the periphery of the pellets, but a large part of the compounds they form are in gaseous state in the hot temperatures areas and especially in the columnar grain region. These volatile fission products, essentially cesium, tellurium, and iodine, play a crucial role in the fuel pin performance for they may migrate radially and axially and buildup at some places on the periphery where some may have a corrosive effect on the steel cladding (see Section 2.03.5.3). Due to localized accumulations, for example, on the UO_2 blanket at each end of the fuel column, they may also induce local clad strains. (see Section 2.03.5.2).

Cesium forms several compounds, the stability of which depends on the oxygen potential $\Delta G(O_2)$.[22–24] For low values of oxygen potential (e.g., $\Delta G(O_2) \approx -500$ kJ mol^{-1}) likely to exist at beginning of irradiation in hypo stoichiometric oxides, the most stable compounds from a thermodynamic point of view are CsI > Cs_2Te > Cs_2UO_4 or Cs_2MoO_4 (depending on the temperature and oxygen potential). The yields of iodine and tellurium are much lower than the amount of cesium (only ~9% for I and 32% for Te); therefore, at low burnup and low $\Delta G(O_2)$, all the iodine and tellurium should be associated in stable cesium compounds. The real situation is more complex and strongly affected by radial and axial migration of volatile fission products, resulting in relative fractions that can be locally quite different from the average relative fission yields. Post irradiation examinations hardly found the compounds CsI and Cs_2Te, which are most stable from thermodynamic calculations.

At higher oxygen potentials ($\Delta G(O_2) \geq -400$ kJ mol^{-1}), likely to occur at high burnup, the respective stabilities change: the most stable compounds become CsI and Cs_2MoO_4; therefore, the Cs_2Te compound may dissociate and as a result, the activity of tellurium may sharply increase with potential consequence on FCCI (see Section 2.03.5.3). The cesium molybdate Cs_2MoO_4 melts at 942°C and has a high vapor pressure (10^{-4} atom at melting temperature), which results in radial migration of cesium and molybdenum that leave the central area to accumulate at the periphery, contributing to the formation of a layer between the fuel pellet and the cladding (see Section 2.03.4.4.2).

2.03.4.2.5 Gaseous fission products

The noble gas xenon and krypton play a crucial role in fuel behavior as they are insoluble in the oxide fuel, precipitate as intragranular and intergranular bubbles inducing local gaseous swelling, and most often are released in large quantities in the fuel pin plena, significantly increasing the gas pressure inside the pins (see Section 2.03.4.5).

2.03.4.3 Evolution of O/M Ratio and Oxygen Potential

As a result of fission, two oxygen atoms are released for every heavy atom destroyed. These liberated oxygen atoms may combine with fission products but a large fraction of these fission products (especially noble metals and rare gas) do not accept oxygen. On an average, the two fission products that were produced for every fission are not efficient enough to combine with the two liberated

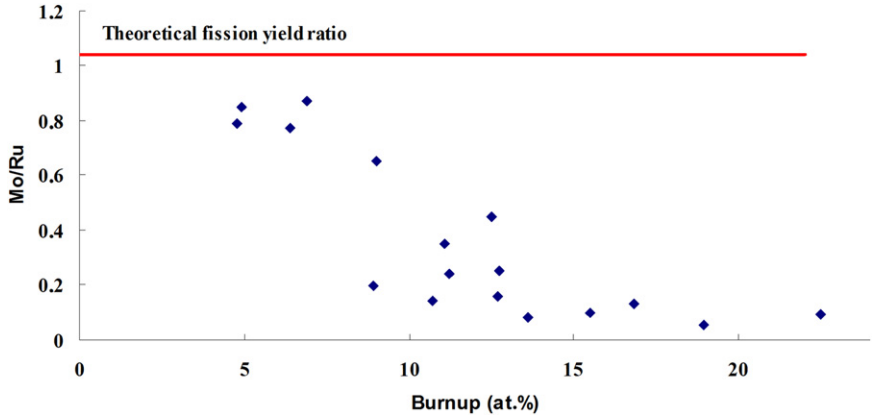

Fig. 9 Evolution with burnup of the Mo content in metallic precipitates in columnar grain region of different Phénix fuel pins with initial O/M ratio of about 1.98.

oxygen atoms, at least as long as the $(U,Pu)O_{2-x}$ fuel remains hypostoichiometric. The excess oxygen dissolves in the fuel matrix where it increases the O/M ratio; fission may therefore be regarded as an oxidizing process.

The oxidation state of fission products can be roughly assessed in the following way:

In the early stage of irradiation of an initially hypostoichiometric fuel $(U, Pu)O_{2-x}$, molybdenum is essentially in a metallic state and a large part of zirconium, alkali metals, and alkaline earths are in solution in the matrix oxide. In these conditions, less than one atom (out of the two fission products) consumes oxygen and the sum of the average valences of the two fission products is about 3–3.3 (to be compared to the mean valence of the fissioned Pu atom, which was near 4). Consequently, the oxide O/M ratio (M stands for U + Pu + fission product dissolved in the matrix) increases at a rate of about 0.003–0.005 per at%, inducing an increase of the oxygen potential of the fuel. This remains valid as long as the molybdenum is in the metallic state.

When burnup increases, an increasing fraction of alkaline and alkaline earths form second phases, and when $(U, Pu)O_2$ approaches stoichiometric composition, the oxygen potential in the fuel reaches values where molybdenum starts to oxidize as MoO_2 (where Mo is tetravalent) or Cs_2MoO_4 (where Mo is hexavalent). This effect appears clearly when analyzing the Mo content in the metallic precipitates of the central region of the pellet by EPMA (**Fig. 9**).[25,26] With initial O/M ratios of about 1.97–1.98, Mo is predominantly in the metallic state up to a burnup threshold between 5 and 10 at% (depending on the initial O/M ratio). A sharp decrease of the Mo content inside the metallic inclusions appears at this burnup threshold: Mo migrates outside the metallic precipitates and at higher burnup, Mo is predominantly in oxidized state.

Therefore, at high burnup (≥10 at%), because of the oxidation of molybdenum, the average valence of the two fission products reaches a value of about 4. Fission products appear able to consume the two oxygen atoms liberated each fission. Due to uncertainties in the chemical state of the different fission products, it is not possible to determine whether there is still an evolution of O/M ratio at a much slower rate, allowing the fuel to enter into the hyperstoichiometric range. Thanks to the buffer role of molybdenum, it is likely that at high burnup, the fuel remains at an O/M ratio not far from 2.00.

This O/M ratio evolution of course induces an increase in the oxygen potential. During the early stage of irradiation, the plutonium valence steadily rises from its as-fabricated value toward the limiting value of 4. This increase in oxygen potential has been demonstrated experimentally: $\Delta G(O_2)$ of fuels irradiated in Phénix up to 11 at% have been measured by an electrolytic cell.[27]

The results (**Fig. 10**) clearly show the increase of $\Delta G(O_2)$, which is associated to an increase of O/M ratio at low burnup. But, even at high burnup, when the O/M ratio remains more or less close to 2.00, the oxygen potential still slightly increases. The introduction in the matrix oxide of RE atoms that are generally trivalent induces an increase of the oxidation state of the remaining actinide cations.

The increase of O/M ratio has a beneficial effect on the thermal conductivity; it partially compensates, at least at low burnup, the thermal conductivity degradation induced by irradiation. But the increase of $\Delta G(O_2)$, which reaches high values (≥ -400 kJ mol^{-1}), has a deleterious effect on FCCI (see Section 2.03.5.3).

2.03.4.4 Migration of Fission Products

2.03.4.4.1 Radial migration

The volatile fission products (Cs, Te, I) have no stable compounds allowing them to remain in the hot regions of the pellets. Above a threshold temperature of about 1200°C, they behave more or less like gas and a fraction of them migrates down the thermal gradient and condensates in the colder area at the periphery of the pellets; in the hot columnar grain region, this radial migration is almost complete. Radial migration concerns not only the fission products classified as volatiles but also some other fission products with high vapor pressure or that may form compounds with high vapor pressures. The metallic fission product palladium has high vapor pressure (10^{-2} Pa at 1500K) and partially escapes pellet central zone migrating toward the outer zone.[25] At high burnup, oxide fuel reaches high oxygen potential and molybdenum transforms into oxidized forms, some of them, especially

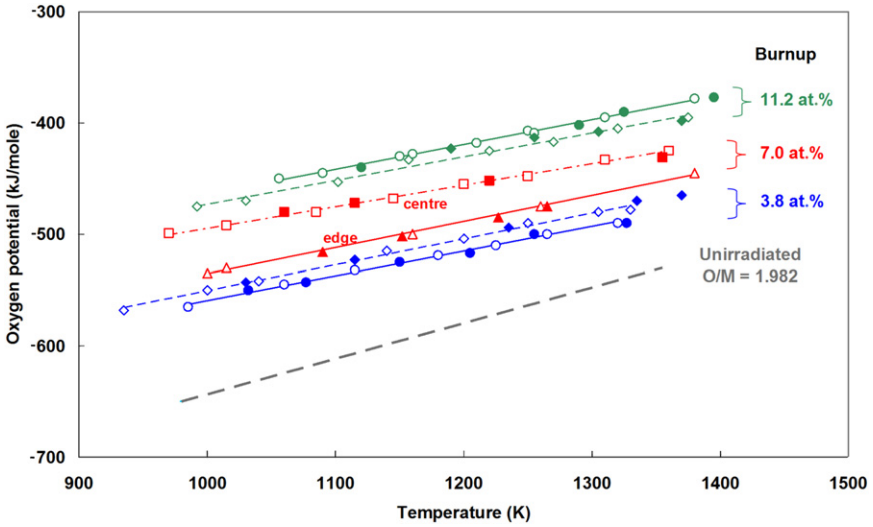

Fig. 10 Evolution with burnup and temperature of the oxygen potential of fast reactor oxide fuels irradiated in Phénix. Reproduced from Matzke, H.J., Ottaviani, J.P., Pellotiero, D., Rouault, J., 1988. J. Nucl. Mater. 160, 142–146.

Cs_2MoO_4 and MoO_3, having high vapor pressure, which explains how Mo migrates to pellet periphery, forming one of the joint-oxyde-gaine (JOG) components. Similar behavior is found for some barium and cadmium compounds.

2.03.4.4.2 Evolution of fuel to cladding gap – JOG formation

At low burnup, between the fuel pellets outer surface and the cladding inner surface, there is a gap filled with gas (mainly helium at the beginning of life, then rapidly a mixture of helium and fission gases when gas release has started). The gap width progressively decreases due to fuel swelling; after a small burnup (a few at%), the gap is practically closed at least in the region of peak power node. However, even after gap closure, there remains a residual gap a couple of micrometers wide due to surface roughness. At high burnup, radial micrographs show a reopening of the gap (see **Fig. 11** giving the evolution of gap width measured in Monju type pins irradiated in Joyo); however, at this time, this gap is no longer filled with gas, but with fission product compounds.

All the fission products migrating toward the cold region of the pellet accumulate first in the oxide fuel, and then escape the fuel and accumulate between the fuel and the cladding where they form a bonding layer (called JOG, joint-oxyde-gaine). At high burnup (>10 at%), this JOG reaches a diameter width of about 150 μm in unstrained pins, but up to more than 300 μm, in pins with high swelling claddings.[28–30] The JOG appears first in the upper half of the fissile column where the fuel surface temperature is the highest; then it evolves progressively toward the lower part.

As revealed by EPMA observations (**Figs. 12** and **13**), this JOG contains predominantly the elements molybdenum, cesium, and oxygen. Other fission products in smaller quantities are also observed in this layer: barium (but no zirconium), as well as palladium, tellurium, and cadmium. Generally, when the JOG is well defined, neither uranium nor plutonium is detected inside. In the upper part of the fuel column where some cladding corrosion has taken place, major elements coming from the cladding (Fe, Ni, Cr) can be found.

The exact composition of JOG is not well known, and it varies axially and even azimuthally according to local temperatures, oxygen potential, and piling up of fission products after radial and axial migration. According to EPMA observations and thermodynamics calculations, the main component of JOG is probably cesium molybdate: Cs_2MoO_4, but a great number of other volatile fission product compounds contribute to the formation of this layer.

At high burnup, this JOG plays a crucial role in fuel pin behavior:

- The thermal conductivity of cesium molybdate Cs_2MoO_4 has been measured by the laser flash method and lies in the range 0.3–0.5 W m^{-1} K^{-1} at operating temperatures,[31] a value 5–10 times lower than the thermal conductivity of $(U, Pu)O_2$, but much higher than the thermal conductivity of a mixture of xenon and krypton at 1000K (0.05 W m^{-1} K^{-1}). Therefore, the heat transfer between the fuel and the cladding is still much better through this JOG than through an equivalent gap filled with fission gases, but not as good as in case of a closed gap when the oxide fuel is in contact with the cladding. Furthermore, the layer is probably not dense and uniform everywhere; in the hottest regions of the JOG, some fission product compounds might migrate by evaporation condensation, leaving behind voids that locally deteriorate the heat transfer,
- From a mechanical point of view, the JOG acts as a buffer (**Fig. 13**). At nominal operating temperatures, most fission product compounds in the JOG are viscous (even liquids for some of them). In case of FCMI, the fission product compounds in the JOG at the level of maximum pressure can be axially extruded, thus relieving the stresses induced in the cladding,
- At high burnup in pins with low clad swelling steels, JOG formation is associated with a decrease of pellet diameter. The release outside the oxide matrix of a considerable fraction of fission products induces a sharp decrease of the matrix swelling,[32] and

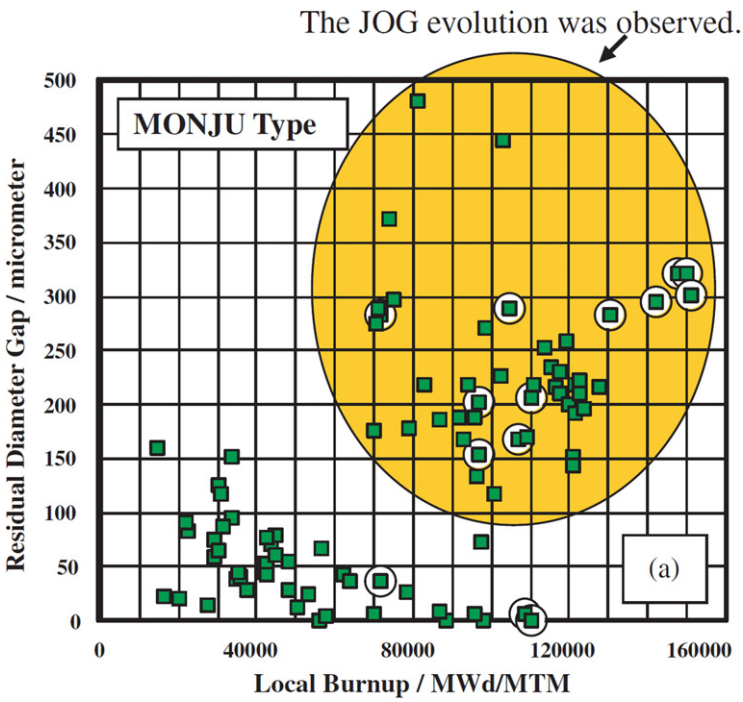

Fig. 11 Evolution with burnup of fuel-to-cladding residual gaps in the Monju type fuel pins. Reproduced from Inoue, M., Maeda, K., Katsuyama, K., Mondo, K., Hisada, M., 2004. J. Nucl. Mater. 326, 59–73.

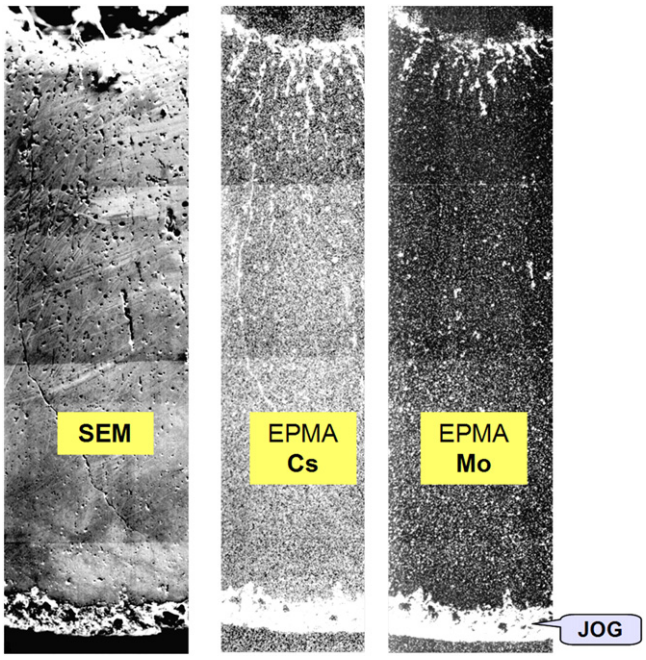

Fig. 12 X-Ray images by EPMA on the JOG in a Phénix pin irradiated at 13.6 at%.

consequently, a decrease of pellet diameter giving room for JOG to form between fuel outer and cladding inner surfaces. However, the overall volume of oxide matrix plus JOG remains more or less constant,

- Fission products in the JOG play a predominant role on FCCI and on the resulting strong corrosion (see Section 2.03.4.3).

2.03.4.4.3 Axial migration

The volatile fission products migrate down the thermal gradient not only radially but also axially. This axial migration starts at beginning of life: the species iodine and tellurium that are created in the hot part of the pellets, the part which undergoes thermal

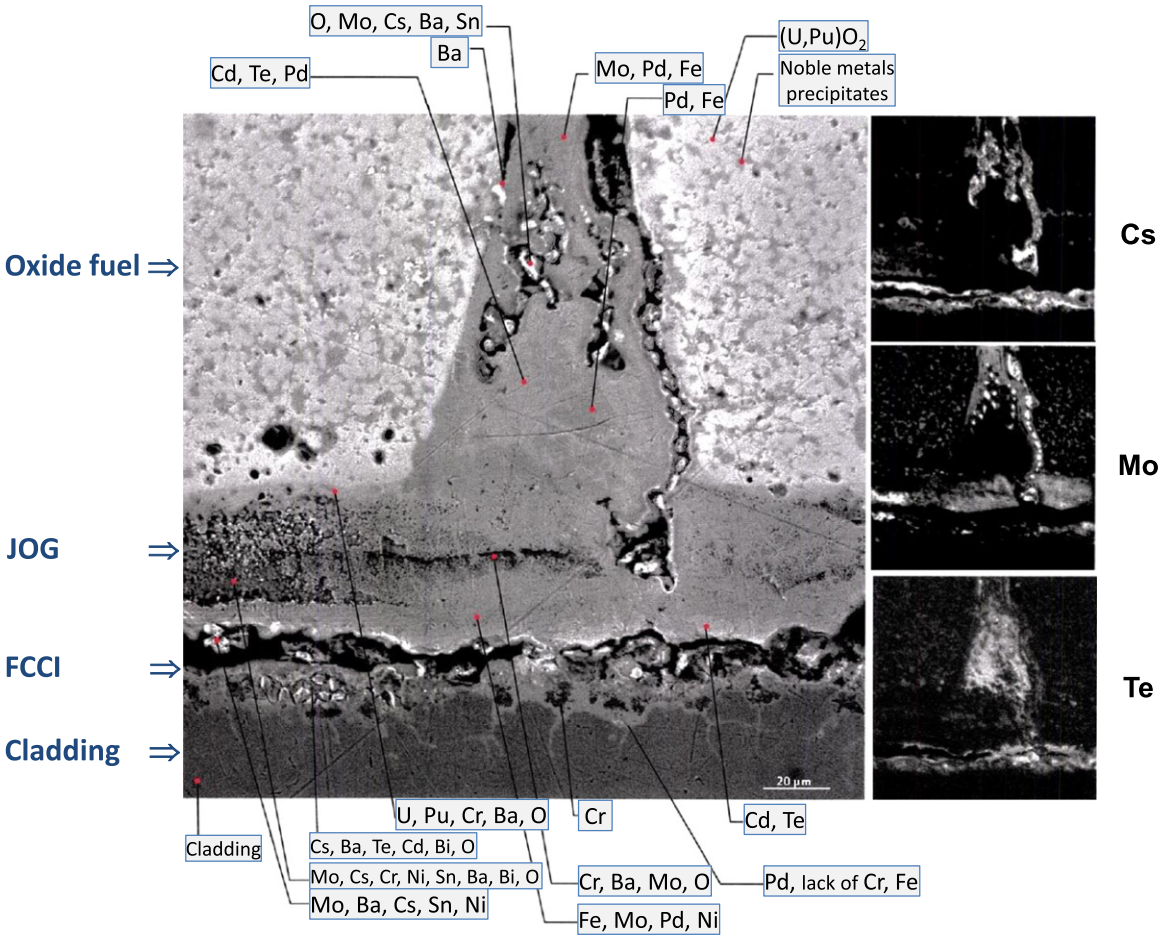

Fig. 13 SEM and EPMA analysis showing on a PFR pin irradiated at very high burnup (23 at%) the wide variety of compounds that enter into the constitution of the JOG.

restructuring, escape the oxide matrix toward the central hole (thanks to pore migration). Then, they migrate and escape the central hole through interpellet spaces, especially those located at both ends of the central hole; axial γ-scanning on pins irradiated during a few days shows this axial migration appearing as peaks of tellurium and iodine at the lower and upper ends of the central hole. In certain circumstances, the piling-up of these corrosive species induces an intergranular clad corrosion (see Section 2.03.5.3.2).

At high burnup, large axial migration of cesium appears on the γ-scanning. In extreme cases, a minimum on the cesium axial profile can be found at peak power node level, that is, at the place of maximum of cesium creation[33] (see, e.g., in Fig. 14 the cesium profile in a PFR fuel pin irradiated at 23 at%).

This cesium migration results partly from migration of Xe isotopes decaying into Cs isotopes (see Section 2.03.4.1) and partly from vaporization – condensation process of all compounds likely to be formed (Cs_2Te, CsI, Cs_2MoO_4, etc.) in hot regions, which migrate toward the colder region radially and also axially. After JOG formation, some evaporation – condensation may occur in the JOG itself; but also every FCMI, for example during power increase, will induce in the JOG an axial extrusion of highly viscous fission product compounds, which will leave the peak power level zone and migrate toward the extremities of the fuel column (Fig. 14).

2.03.4.5 Behavior of Fission Gases

Fission gases are not soluble in oxide and their behavior in nuclear fuels is a topic that has been generating a huge amount of studies for several decades, and a great number of papers have been published in literature predominantly addressing gas behavior in oxide fuels for LWRs. A great difference between LWR fuels and fast reactor oxide fuel has to be kept in mind:

- In LWR rods, the fuel is operating at low temperatures (typically between 500 and 1000°C) and the rods are designed with a small plenum taking into account the observation that, in nominal cases, a small fraction of produced gas is released outside the fuel pellets in the plenum (typically $<10\%$). Therefore, at high burnup (~ 7 at%), UO_2 matrix must retain a significant amount of fission gases because their release may be a limiting factor inducing excessive inner pressure in the rods despite the high coolant pressure,

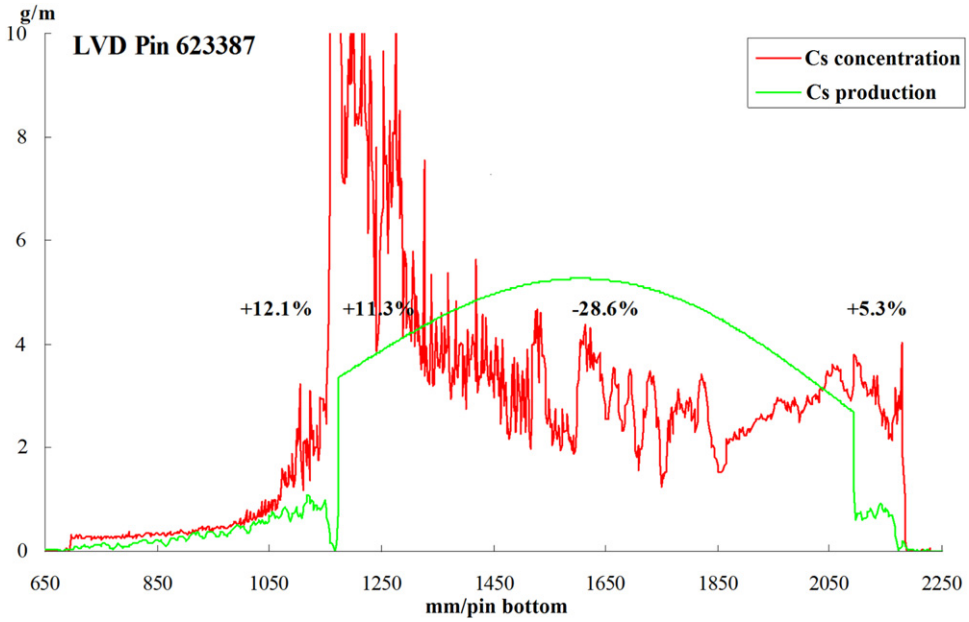

Fig. 14 Gamma-scanning of cesium in a PFR pin irradiated at very high burnup (23 at%).

- On the contrary, in fast reactor oxide fuel pins, because of the high temperatures but also higher target burnups (>10 at%), large gas releases are generally observed; typically, 80%–90% of the production. (Indeed, design calculations generally assume a release of 100%). The design of the pins has to consider this large release, and mixed oxide fuel pins for fast reactors are designed with a large plenum (about the same volume as the fuel column). Therefore, gas release in fast oxide fuel pins is not a limiting factor. Nevertheless, fission gas behavior plays a considerable role in fuel performance as it influences thermal behavior even at low burnups and fuel swelling. In addition, the increase in internal pressure induced by these large releases can lead to cladding deformations by irradiation creep.

2.03.4.5.1 Formation of fission gases

The gaseous fission products are primarily rare gases xenon and krypton in various isotopic forms: ^{129}Xe, ^{131}Xe, ^{132}Xe, ^{134}Xe, ^{136}Xe and ^{83}Kr, ^{84}Kr, ^{85}Kr, ^{86}Kr. Helium (^{4}He) is also produced in oxide fuel by ternary fissions, (n,α) reaction on oxygen, and predominantly during irradiation by α-decay of some actinide isotopes, mainly ^{242}Cm plus ^{238}Pu, and ^{241}Am. A specificity of helium is that it continues to be produced after reactor shutdowns and during fuel storage through the α-decay production.

The elemental yields of these gases are ~0.23 atom per fission for xenon, 0.02 atom per fission for krypton. This corresponds to a production of Xe + Kr of about 0.21 cm^3(NTP) g^{-1} per at%. The exact values depend on the neutron flux spectrum, on plutonium enrichment and its isotopic composition and it evolves with burnup. The fission gas yield in a fast reactor (~0.25 (Xe + Kr) per fission) is still lower than that in a thermal reactor (~0.31 (Xe + Kr) per fission), because in thermal spectrum, the capture cross-section of ^{135}Xe is so high (10^6 barns) that, before decaying into cesium, ^{135}Xe mostly transmutes into ^{136}Xe, which is almost stable.

With a plutonium resulting from the reprocessing of low-irradiated fuels characterized by a plutonium isotopy with a high proportion of ^{239}Pu and a very low ^{238}Pu one (For example, the reprocessing of the French UNGG fuels with which were manufactured the mixed oxides of French SFRs), the production of helium in (U, Pu)O_2 fuels is about 0.01 atom per fission (~0.01 cm^3 (NTP) g^{-1} per at%). As the fuel pins are initially filled with helium, the influence of this small helium production on the behavior of standard fuels remains low. It is not the same with fuels made with plutonium from reprocessing of LWR fuels (UO_2 and MOX) and also for fuels containing some percent of MA, especially americium. For these cases, helium production is much higher (from 5 to 10 times more) and its own behavior must be taken into account.

2.03.4.5.2 Fission gas release

The behavior of fission gases is complex. Given their very low solubility in oxide fuel, fission gases tend to diffuse within the grains and precipitate as small intragranular bubbles (some nanometers). Fission fragments can redissolve the precipitated gas. Bubbles grow by trapping gas atoms and vacancies; they coalesce when two bubbles meet; they migrate randomly and up the thermal gradient (by vaporization–condensation, surface diffusion, or volume diffusion, depending on temperature and bubble size). Most gas reaches grain boundaries either by atomic diffusion or by migration of intragranular bubbles. On the grain boundaries, gases precipitate as elongated intergranular bubbles, which grow and interconnect, finally allowing venting of the gas toward all free volumes of the pin (central hole, fuel cracks, fuel to cladding gap and lower and upper plena) through open porosity and interlinked intergranular bubbles.

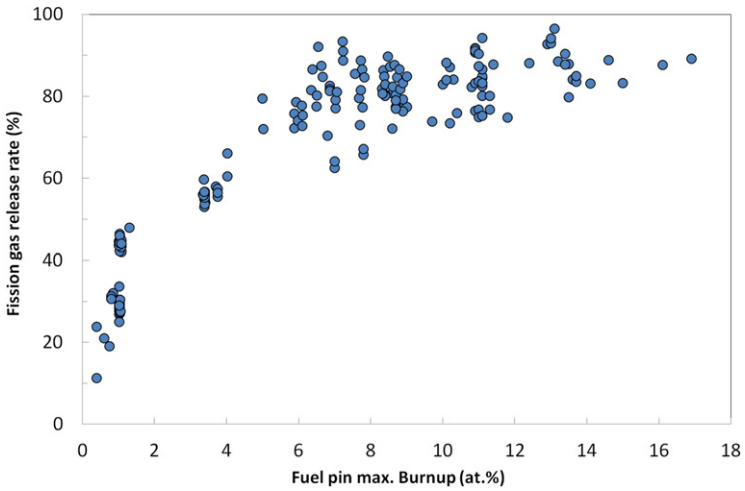

Fig. 15 Evolution with burnup of global fission gas release in standard Phénix pins.

Puncture tests of irradiated fast fuel pins allow the determination of the overall gas release in the free volumes. As an example, Fig. 15 gives the fractional release, as a function of burnup, of Phénix pins irradiated in nominal conditions. Even at very low burnup, a significant gas release is already observed (~30%–50%); the gases created in the columnar grain region are almost completely released. The fractional release increases with burnup and, at high burnup (>10 at%), it levels at about 80% in unstrained pins, and 90% in pins with significant cladding diameter deformation. The results clearly indicate that fission gas release is driven by fuel thermal level and by burnup.[34]

Microprobe and SIMS analyzes give information on the radial profile of xenon; sublimation or dissolution of irradiated pellets at several levels of a fuel pin gives the axial profile of occluded fission gases. At moderate burnup (≤7 at%), gas release is essentially a thermally activated mechanism; the release is almost complete above ~1400°C and very low below ~1000°C. Therefore, the fractions of gas release are directly related to the parameters governing the temperature field inside the oxide fuel: initial density and O/M ratio of the pellets, fuel to cladding gap size, linear heat rate, but also clad diameter deformation for materials that swell early such as 316 (SA) steel which has the effect of re-opening the gap, etc.

At a threshold burnup of about 7–9 at%, the microstructure changes at the periphery of the pellets; the grains (initially ~10 μm) subdivide into smaller grains (~1–2 μm) and a precipitation of bubbles occurs (see Fig. 16).

This transformation is quite similar to the restructuring observed, at about the same burnup but at lower temperatures, at the periphery of pellets and in the plutonium rich agglomerates of the LWR MOX fuel rods and known as 'Rim effect' or 'high burnup structure (HBS)'.[35–37] At about the same burnup, the JOG is formed (see Section 2.03.3.4). Results of sublimations (Fig. 17) show that, at a given level of fuel pins irradiated under steady-state conditions, the amount of fission gas occluded in fuel pellets increases with burnup up to a burnup threshold (~5–8 at%) and suddenly drops at about the same time as JOG forms and fuel restructures at the periphery.

This drop may be partly due to fuel overheating induced by clad swelling, but this probably means also that, at high burnup, even the low-temperature region of fuel pellets releases a fraction of its fission gases; oxide cannot accumulate fission gas beyond a certain level. (Contrary to what happens in the HBS zone of LWR fuels, where most fission gases are still present after restructuring. But the temperatures in the outer zone of fuel pellets are typically 700–1000°C in fast oxide fuel, much higher than in LWR fuel where the HBS zone undergoes temperatures of about 450–650°C.)

2.03.4.6 Fuel Swelling

Burnup induces an increase in the number of atoms inside the fuel. 10 at% burnup corresponds to 10% increase in the total number of atoms (heavy atoms + fission products). As a direct consequence of this increase, a fuel swelling is observed; its volume increases with burnup. The two atoms produced each fission occupy on average more space than the initial plutonium atom.

Density measurements carried out on irradiated fuel pellets give access to this overall volume change. Hydrostatic densities of irradiated fuels show a linear decay with a slope of about 0.7% per at%. After correction of the mass of gas released by the fuel, a swelling rate of about 0.6% per at% can be inferred from this density slope. This swelling rate, which seems to remain constant up to very high burnup (20 at%), integrates all the effects: volume change of oxide matrix, volume of metallic phase and oxide phase, volume of JOG at high burnup, and a certain contribution from gaseous swelling. It is an average value, and significant variations may be encountered due to radial and axial migrations of fission products. Especially cesium, which displays large radial and axial migrations, plays a considerable role on fuel swelling, and a strong relationship may be established between local swelling and cesium amount; swelling is lower than expected at levels where cesium profile is depleted (see Fig. 14).

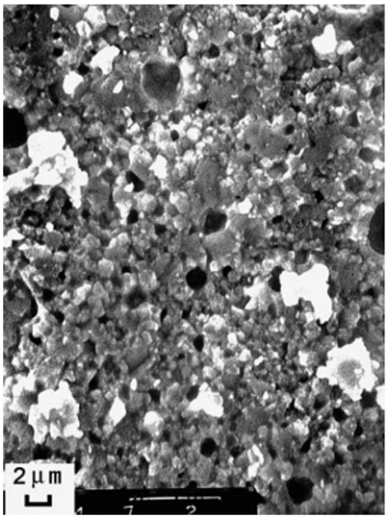

Fig. 16 SEM Fractograph of a porous rim structure at the periphery of a mixed oxide fuel pellet irradiated in SFR at 97 GWd/t (~10 at%). Reproduced from Roche, L., Pelletier, M., 1999. Modeling of the thermomechanical and physical processes in FR fuel pins using the Germinal code. In: Proceedings of the International Symposium on MOX Fuel Cycle Technologies for Medium and Long-Term Deployment (IAEA-SM-358/25), May 1999, 17–21. Vienna, Austria.

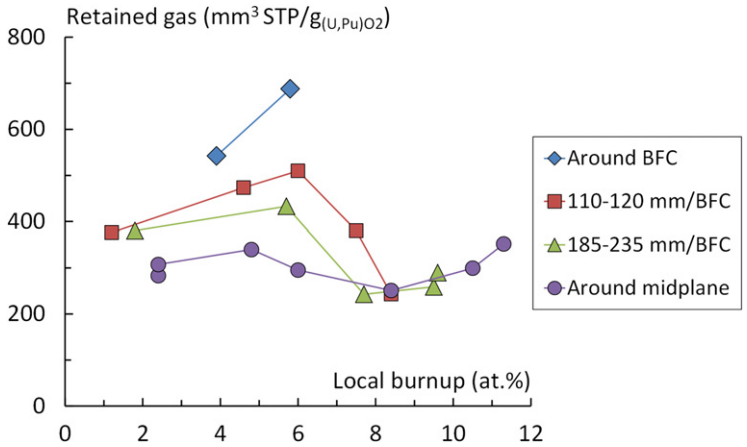

Fig. 17 Evolution with the axial position and the burnup of fission gas retention in Phénix fuel pins.

Two different types of swelling are often considered: the solid swelling due to fission products (FPs) in solid state and the gaseous swelling. The respective contributions of each type of fission product to the fuel solid swelling can be assessed considering the volume V_i occupied by each family of fission product and reporting it to the atomic volume of the plutonium V_{Pu}[1]:

- FPs in solid solution are in substitution to the actinide atoms ($V_i/V_{Pu} = 1$). At high temperature as it is the case in fast oxide fuel, the lattice parameter of the matrix slightly decreases with burnup ($\sim -0.007\%$ per at%),
- FPs pertaining to the "noble metal" family have an atomic volume lower than actinide atom ($V_i/V_{Pu} \sim 0{,}36$),
- The same occurs for volatile FPs whose average volume gives about ($V_i/V_{Pu} \sim 0.76$),
- On the contrary, FPs forming oxide precipitates have a larger volume ($V_i/V_{Pu} \sim 1.74$).

Taking into account the elemental yield of each FP family (see **Table 2**), a solid swelling rate of about 0.3 ($\pm$ 0.15)% per at% can be inferred from the above values. This rate is slightly lower than the swelling deduced from density measurements: retained fission gases bring an additional contribution to swelling rate.

In steady-state conditions, at high burnup, as most fission gases have already been released, and as fuel swelling is slightly constrained by the cladding, the gaseous swelling rate is low. (This is one of the great advantages of oxides over other ceramic fuels as carbide or nitride or metallic fuels, which have a much higher swelling rate, due to gaseous swelling, inducing strong loadings to the cladding in the case of ceramic fuels.) However, during any situation when oxide fuel is no longer in mechanical interaction with its cladding, the gaseous swelling rate may considerably increase.[38] This occurs, for example at low burnup, when gaseous swelling contributes to gap closure (See section 2.03.3.4.1). This happens also at the locations in the fissile column where the clad swelling causes large clad

deformation causing both temperature increase and pressure drop induced by the re-opening of the gap; consequently, gaseous swelling strongly increases and helps to avoid a too large re-opening of the fuel-to-cladding gap and prevents overheating of the fuel.

2.03.5 Limiting Phenomena

Let us first recall that during the past decades, strong cladding deformation, up to 10% increase, due to swelling of austenitic stainless steel has been the main limiting factor for the performance of oxide fuel pins in fast reactors. Experience on in-pile behavior of fast fuel pins has been mainly achieved with pin claddings in austenitic stainless steels, and the limit burnup was determined by an excessive clad deformation due to swelling of the clad material, induced by the high fluence of fast neutrons and high irradiation dose (>100 dpa NRT). Improvements of steel composition and metallurgical state (316 in solution annealed (SA) or cold worked (CW) state, then CW 316 Ti and 15/15 Ti) progressively allowed increasing the dose beyond 100 dpa NRT and therefore the burnup. But, the main cause of failure in these pins remained associated to large clad swelling generating large clad deformation ($>5\%$ diametral) and interaction between pins in the bundle. Large volume swellings (≥ 6 vol%) were also generally associated with embrittlement of the clad Austenitic steel.

Other types of alloys with higher resistance to swelling have been tested, especially nickel alloys, such as Inconel 706 (France and USA), or Nimonic PE16 (UK) and ferritic–martensitic steels, such as EM12 (France) or HT9 (USA). But, the most promising alloys that are currently considered for the future are the ferritic–martensitic steels reinforced by a nano dispersion of oxide precipitates: ODS alloys (Oxide Dispersion Strengthened).[39] The behavior of these materials under irradiation damage is described in other parts of this book.

Besides this limitation due to clad behavior, the oxide fuel itself may bring some limitations related to thermal, mechanical, and chemical behavior.

2.03.5.1 Margins to Fuel Melting

Many experimental results have shown that significant fuel melting can occur in an irradiated fuel pin without inducing a clad failure. It is generally considered that, provided there is enough volume to accommodate thermal expansion, a significant fraction of molten fuel in the oxide pin (up to $\sim 20\%$ depending on initial smeared density and burnup) would not induce any apparent harmful consequence. For example, in FFTF, the experiment DEA-9 has demonstrated that a once-molten fuel (melting up to half the pellet radius at beginning of life) was able to reach high burnup.[40]

Nevertheless, in order to keep a large margin to any uncontrolled phenomenon such as axial movements of fissile nuclides, fuel licensing requires guaranteeing the absence or a small fraction of fuel melting in all the nominal operating situations. As the nominal oxide temperatures are high, and as all the uncertainties have to be taken into account, this conservative requirement induces a strong constraint on the maximum linear heat rating achievable.

2.03.5.1.1 Temperature field in the oxide fuel

The temperature at first rise to full power is often the highest center temperature achieved during the life-time of oxide fuel in reactor, especially in solid pellets. The phenomena occurring in the hours and days following this first rise to full power induce globally a sharp decrease (several hundreds of degrees) of this temperature:

- Radial redistribution of oxygen improves fuel thermal conductivity in the periphery, where thermal flux is the highest,
- Fuel restructuring decreases fuel porosity; and formation of the central hole (or enlargement of the central hole in case of annular pellets) decreases the center temperature. These favorable effects of fuel restructuring on temperature may be somewhat altered due to a possible increase in the plutonium content at the edge of the central hole and its impact on the decrease of the solidus temperature of the mixed oxide,
- Gap closure has the strongest effect: thanks to the enhancement of fuel to cladding heat transfer, fuel temperatures may decrease by several hundreds of degrees.

At higher burnup, the general trend is to increase the fuel temperature for the following reasons:

- Xenon has a much lower thermal conductivity than helium; thus, release of fission gases induces a degradation of the conductivity of the gases in the residual gap, with a deleterious effect on the heat transfer between fuel and cladding,
- As an effect of burnup, fuel thermal conductivity is continuously decreasing; all defects and fission products act as diffusion centers for phonon,
- In case of clad deformation, at medium or high burnup, the tendency is to reopen the gap, inducing a degradation of the fuel to cladding heat transfer. However, at the beginning of JOG formation, this heat transfer is improved because of the replacement of a gaseous gap with very low thermal conductance by FP compounds with higher thermal conductivity. Nevertheless, the low conductivity of cesium molybdate (see Section 2.03.4.4.2) and the increase of its thickness up to 300 μm have the effect of degrading again the fuel to cladding heat transfer,

This general trend to temperature increase with burnup is partly compensated by the continuous decrease of linear heat rating in most of the fuel pins as evident from past experience worldwide. For plutonium content of the oxide greater than 20% which is

a usual value for medium size reactors like Phénix, typically, LHR at peak power node were above 400 W cm^{-1} at beginning of life and around 300 W cm^{-1} at high burnup. As a result, it was generally calculated that the maximum center temperature of the fuel was seen at the very beginning of life, even if the center temperature at end of life was not far from this maximum value.

This is would be likely to change in the future: in order to increase the safety characteristics and especially to limit excess reactivity of the core of sodium-cooled fast reactor of Generation IV design, the trend would be to use large diameter pins with lower plutonium content (around 15% for a homogeneous core such as Superphénix) allowing an internal breeding compensating the plutonium consumption.[41] As a result, the LHR would remain almost constant during the whole in reactor life. Therefore, the maximum temperature would probably occur at end of life. This would then have to be taken into account for the choice of the maximum reference LHR of the reactor fuel pins.

2.03.5.1.2 Nominal situation and case of control rod withdrawal

In fast oxide driver fuel pins, typical maximum center temperatures lie in the range 2000–2200°C for nominal conditions, up to 2400°C in some cases. The solidus temperature of as-fabricated (U, Pu)$O_{2.00}$ is 2782°C for a plutonium content of 20% and 2751°C for 30%. This melting temperature of mixed oxide decreases with deviation from stoichiometry (~ -50°C for $MO_{1.95}$ as compared to $MO_{2.00}$), and decreases also with burnup (~ -34°C for 10 at% burnup).

Therefore, when the center temperature is calculated with nominal values of the parameters and on a best-estimate basis, the margin to fuel melting reaches several hundreds of degrees centigrade. However, when taking into account all the uncertainties on fabrication parameters (cladding and pellet diameter, pellet density, O/M, Pu content), on fuel properties (thermal conductivity), and operating conditions (linear heat rating, cladding temperature), the resulting uncertainty on the maximum center temperature is rather high ($\sim$100°C for one standard deviation). Moreover, this absence or insignificant fraction of fuel melting must remain guaranteed even during some off-normal situations such as control rod withdrawal, when LHR may increase about 7% before reactor undergoes a scram.

At high burnup, the center temperatures are calculated with higher uncertainties because of degradation of thermal conductivity of the irradiated fuel, uncertainties on the heat transfer across the JOG, and activation of mechanisms such as gaseous transient swelling during power increase. In order to validate code calculations, several experiments have been performed, either on pins instrumented with a thermocouple inside the central hole, or on pins irradiated at high linear heat rating in order to generate a limited fuel melting. The radius of molten fuel is then used to validate calculations. For example, the JOG1 and the JOG2 tests were power-to-melt experiments (up to 770 W cm^{-1}, 20% molten fuel) performed in Cabri on Phénix pins irradiated up to 15 at%.[42] Results of post irradiation examination showed a decrease of JOG width at peak power node due to axial extrusion toward fuel column ends of the viscous compounds of fission products filling the JOG. Such experiments provide data enabling to validate the models of heat transfer across the JOG and the mechanism of gaseous transient swelling in the pellets. Before melting occurs, this transient swelling may reduce the central hole diameter at a rate depending on the kinetics of power rise and amount of occluded fission gas. This results in a decrease of the power-to-melt, as a consequence of central hole reduction or closing and increased porosity in the central region.

2.03.5.2 Fuel Cladding Mechanical Interaction

In the early days of development of fast oxide fuel, fuel cladding mechanical interaction (FCMI) was considered as a mechanism likely to induce strong limitations both on burnup and on operating conditions. Indeed, in other families of fast fuels and especially in carbide and nitride fuels, FCMI revealed to be a major limiting factor and the predominant cause of fuel pin failure; this is due to the high swelling rate of these fuels and to their low creep rate at operating temperatures. In oxide fuel pins, thanks to the low swelling rate of oxide and to its high fuel creep rate related to its high temperature, FCMI does not play such a crucial role; it has nevertheless to be taken into account both in the fuel pin design and in the operating conditions.

2.03.5.2.1 Limit burnup due to FCMI during steady-state operation

During irradiation, the oxide fuel swells at about 0.6% per at% (see Section 2.03.4.6). Consequently, theoretically the volume of a fuel that reaches a burnup of 15 at% has increased by about 9%. As the temperature is much higher in the oxide than in the cladding, fuel thermal expansion is larger than cladding expansion and this consumes 1%–2% of the initial free volume. Post irradiation examination shows that a porosity of several percentages always remains in the pellet. When designing the fuel pin, a free volume has to be managed, which considers fuel swelling, differential thermal expansion between fuel and cladding, and residual porosity.

Several experimental programs and calculations have been carried out worldwide in order to determine the optimized smear density of fuel pins as a function of target burnup and to analyze the potential risks of clad strain and damage induced by FCMI, for example, Gatesoupe *et al.*[43] Biancheria *et al.*[44] Levine *et al.*[45] Dienst *et al.*[46] It appeared that very high smear densities ($\geq$ 90% TD), and especially narrow fuel-to-cladding gaps, should be avoided; in such pins, FCMI may induce additional clad strain.

For intermediate smear density (between 85% TD and 90% TD), the situation is not straightforward: driver fuel pins of Phénix and FFTF, which were in this family (88% TD for Phénix, 86% TD for FFTF), have been able to reach high burnups (beyond 15 at%) without reaching a limit due to consumption of available free volume for accommodation of fuel swelling. But, in most cases, these pins had clads with steels undergoing irradiation swelling, which provided additional free volume at high burnup. From immersion density measurements on clad and analysis of clad deformation, it was deduced that clad deformations are mainly due to steel swelling

and that plastic strain of clad (the part of deformation that is not due to swelling) results essentially from irradiation creep of steel induced by the high inner pressure due to fission gas release and not by FCMI.

One can also refer to the results of fuel pins irradiated in PFR[47]: despite rather high smear density (86% TD and 88% TD) and low clad swelling (diameter clad deformation of the nickel alloy Nimonic PE16 was less than 1%), very high burnups were achieved (23 and 19 at%). And the FCMI contribution to clad deformation remained small and localized in the lower part of fuel column where a strong accumulation of cesium is observed (see **Fig. 14**).

In fuel pins with annular pellets and clad with irradiation swelling, the diameter of the central hole at high burnup is generally larger than its initial value. In case of clads with very low swelling, a small decrease of the central hole diameter may be observed in the lower and the upper parts of the fuel column, this diameter nevertheless remaining very close to its fabrication value.[42]

In fast oxide fuels, this benign effect of FCMI during steady-state operation is a consequence of the following points:

- Low swelling rate of oxide (as compared to carbide or metal fuels),
- high fuel temperature that allows high creep rates. Even in the outer part of pellets, thermal creep and irradiation creep in oxide fuels relieve the FCMI stresses induced by fuel swelling. As long as a central hole is available, calculations account for a hoop stress not exceeding a couple of MPa induced in the cladding by FCMI during steady-state operation,
- JOG formation and axial migration of cesium and other fission product compounds. Swelling rate of (U, Pu)O_2 itself is lower than 0.6% per at%; and volume increase due to JOG formation can hardly strain the clad as the fission product compounds of the JOG have no real mechanical strength.

Nevertheless, despite these encouraging results, designers do not rely on axial migration of cesium to relieve FCMI stresses. For commercial reactors with high burnup targets (15 or 20 at%), it is nowadays considered that reliable fuel pins should be designed with smear density not exceeding 85% TD. This low smear density may be achieved by using either annular pellets or highly porous oxide pellets. Low density of pellets has adverse effects on thermal behavior and on in-reactor stability of the fuel stack. This is why fuel pins of latest commercial fast reactors have been designed with annular pellets (see Section 2.03.7.1).

2.03.5.2.2 FCMI due to power increases

Nevertheless, in some cases, the consequences of FCMI should be seriously considered. Each time the linear heat rate of a fuel pin is increased, if the fuel to cladding gap is closed, the differential fuel cladding expansion induces additional stresses in the cladding. For high LHR, thanks to high fuel temperatures, a thermal creep relaxation quickly operates and the cladding stresses remain low; but if the power increase occurs after an extended period at reduced power, enough period to get a complete gap closure, fuel temperatures at the beginning of power ramp are too low to permit high thermal creep rates and fuel irradiation creep has not enough time to relieve FCMI stresses. In such a case, high stresses may be induced in the clad, exceeding the elastic limit and generating permanent clad strain and a risk of pin failure in case of previous severe cladding embrittlement.

To prevent any risk in such a situation, highly brittle irradiated clad material should be excluded; and the rate of power increase should be limited, relying on calculations by fuel performance codes.

2.03.5.2.3 FCMI due to cesium accumulation

In many pins irradiated to high burnup, diameter profilometries reveal small cladding strain peaks at the level of UO_2 insulator pellets, or in front of the first pellets of the axial blankets, at each end of the fuel column. These strain peaks, clearly associated to cesium accumulation on γ-scanning profiles, result from swelling of fertile UO_2 due to reaction with cesium, forming cesium uranates: Cs_2UO_4 or $Cs_2U_4O_{12}$ for high oxygen potentials,[20,48] or from filling up of the gap at this level by fission product compounds. As fertile UO_2 is much colder than fissile (U, Pu)O_2 and has generally no central hole, this volume increase of UO_2 pellets results in clad strain as there is no possibility for swelling accommodation inside the oxide.

Similar observation of a local cladding strain has also been observed in the fuel column at the level of cesium accumulation. It may be observed either near the ends of the fuel stack, in places where LHR and fuel temperatures are low, or at the level of FCCI where high volume increase is induced not only by accumulation of fission product compounds but also by reaction products resulting from clad corrosion (see Section 2.03.5.3).

2.03.5.3 Fuel Cladding Chemical Interaction

Fuel cladding chemical interaction (FCCI) is a general term for all types of chemical reaction resulting in a corrosion of the cladding inner surface. Indeed, the (U, Pu)O_2 fuel itself does not directly react with the cladding, but it provides the oxygen needed for some of the reactions. It was demonstrated in out-of-pile test that the volatile fission products, tellurium and cesium, are the corrosive species able to overcome the passivation of stainless steel and therefore to induce clad corrosion.

FCCI appears as one of the potential life-limiting factors for high burnup fuel elements. Many studies have been carried out worldwide in order to understand and model this phenomenon: a large number of nondestructive examinations (especially eddy current which allows to localize the clad corrosion and assess its magnitude on a great number of irradiated pins), thorough destructive examinations (especially optical microscopy to measure the corrosion thickness and EPMA to find out the corrosion products resulting from the reaction), thermodynamics studies, out-of-pile tests, and specific irradiation programs.

Although a qualitative understanding of corrosion mechanisms has been achieved, it is not yet possible to give a complete physical description of FCCI and therefore to predict corrosion depths in every circumstance. In fact, there is not only one corrosion mode, several types of reactions and mechanisms are possible, occurring at different stages of irradiation, sometimes successively in the same pin, and resulting in different attack features. The occurrence of one or another mechanism depends upon local conditions: clad and oxide temperatures, temperature gradient across the fuel-to-cladding gap, oxygen potential, and relative amounts of the different corrosive species (Te, Cs, I) and other fission products (especially Mo) involved in the equilibrium of the main chemical reactions. These local quantities of fission products depend not only on their respective yield; they result from their radial and axial migration, and their local buildup is related to the different chemical reactions likely to occur between fission product compounds, fuel, and cladding components.

The equilibrium of these different reactions is very sensitive to local conditions and determines the activity of corrosive species. This explains why a large scatter of corrosion depths may be observed in similar fuel pins, and why a great variety of FCCI features has been observed. Local conditions depend on initial characteristics (such as O/M ratio) and operating conditions (such as linear heat rate), and evolve during pin time-life in reactor (e.g., clad deformation modifies fuel surface temperature and therefore oxygen potential).

We present hereafter some of the main types of FCCI effects.

2.03.5.3.1 Early-in-life corrosion

In a few cases, irradiated oxide fuel pins exhibited severe intergranular corrosion on the inner cladding surface, which could be observed at very low burnup (after only one or two weeks of irradiation).[4,5] Such attack occurred essentially in highly rated pins ($\geq$450 W cm^{-1} at beginning of life), and it induced clad failures in some cases, especially in solid pellet fuel pins irradiated in Rapsodie after up rating into Fortissimo.

Out-of-pile tests on corrosion by cesium and tellurium and thermochemical evaluation reveal that an intergranular attack of stainless steel claddings may occur when the Cs/Te ratio is lower than 2.[49,50] In such a case, tellurium activity is no longer buffered by formation of the very stable compound Cs_2Te and free tellurium is available for fission product-induced liquid metal embrittlement. As cesium fission yield is about six times higher than tellurium yield, such a low Cs/Te ratio is not found at moderate or high burnup.

However, at beginning of life, the Cs/Te ratio is much lower than the equilibrium value because of the effect of radioactive decay chains; during the first week of irradiation, tellurium may be locally in excess. In pins irradiated under high linear heat rates, and therefore generating high fuel temperatures, tellurium and iodine generated in the columnar grain zone escape from the oxide fuel and build up on the cladding. γ-Scanning on such pins shows peaks of tellurium and iodine in front of oxide interpellets at the top and the bottom ends of the central hole.[4] If the oxygen potential and the clad temperature are high enough, an intergranular attack of stainless steel may occur probably by formation of chromium telluride (Cr_2Te_3) at grain boundaries with a regeneration process of the small quantity of tellurium.

In order to prevent this early-in-life corrosion, one solution successfully applied in Rapsodie and Phénix is to limit the LHR during the first days of irradiation, thus reducing escape and accumulation of corrosive fission products while tellurium is in excess. At similar LHR, the use of annular pellets which significantly lowers fuel temperatures also seems to reduce this risk of early-in-life corrosion.

2.03.5.3.2 Intergranular corrosion

Intergranular corrosion has been also observed in a lot of oxide pins at moderate burnups, and again associated with high fuel temperatures related to high LHR, low fuel density, or vibropacked oxide fuels. Such a corrosion mode is probably linked to high-temperature gradients across the fuel-to-cladding gap, enabling the cesium pressure in equilibrium with cesium uranate formation on the fuel surface to become higher than the cesium partial pressure required for cesium chromate formation on the cladding inner surface.[51] In order to prevent this corrosion mode, very high fuel surface temperatures should be avoided. Another way is to reduce the oxygen potential by using low O/M ratio, but with adverse effects on fuel temperatures.

Vibropacked oxide fuel pins exhibited such an intergranular corrosion when irradiated at a high LHR. This occurred especially in vibropacked fuel pins irradiated in the experimental reactor DFR.[52] To avoid this corrosion in vibropacked mixed oxide fuel pins irradiated in Russia, several percentages of uranium metal powder are added to the fissile mixed oxide in order to decrease the oxygen potential.[8]

2.03.5.3.3 Corrosion at high burnup

Clad corrosions observed at high burnups appear generally as a rather uniform broad-front layer sometimes preceded by a small intergranular attack; it may reach considerable depth. The Phénix pins irradiated at high burnup give typical examples of this FCCI mode. Clad corrosions are located in the upper third of the fissile stack and affect a large clad surface; several tens of millimeters long and more or less azimuthally uniform. As an example, **Fig. 18** shows one of the largest corrosions observed in Phénix pins, up to 200 μm deep, i.e., more than 40% of the initial cladding thickness.

During nondestructive examination, such corrosion may be detected and localized by eddy currents. It is often associated to cesium accumulation seen on the γ-scanning, and in some cases, but rarely, to small localized cladding strain peaks (cf. Section 2.03.5.2.3).

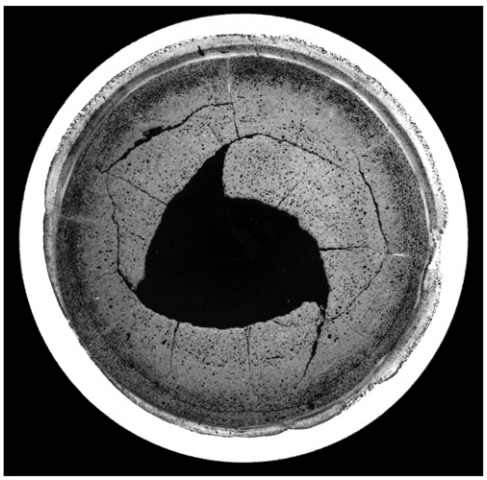

Fig. 18 Macrograph showing a strong FCCI observed in a Phénix pin irradiated at 17 at% (The central fragment was pulled out during sample preparation).

Burnup plays a crucial role in the development of this corrosion, which is directly linked to the amount of created corrosive species, which is also linked to the high oxygen potential needed for this corrosion to occur. A minimum clad temperature is necessary; this is why corrosion is not observed in the lower half of the fuel column.

Cladding strain plays an indirect role; most extensive corrosion has been observed in pins clad with austenitic stainless steels (as C.W. 316 Ti or C.W. 15/15 Ti), which exhibited at high burnup (and high dose) a swelling bump in the lower half of the fuel column. This clad deformation induces locally an overheating of the oxide fuel, which favors an axial migration of volatile fission products from the region with high fuel temperature (lower part) to colder areas (upper part with small clad strain), thus locally enhancing the quantity of corrosive species. Consequently, swelling resistant cladding materials such as ferritic steel are likely to be less susceptible to strong FCCI than austenitic stainless steel, but this has yet to be extensively demonstrated at high burnup.

The mechanism of this corrosion involves essentially tellurium and cesium[4,53] and needs local conditions where Cs_2Te compound can split and high tellurium activity may develop. Many types of reactions of cesium and tellurium with oxide fuel, fission product compounds, and clad components are likely to occur depending upon relative amounts of constituents, local conditions of temperatures, and oxygen potential.[54] Among these different reactions, two probably play a crucial role in clad corrosion:

- Reaction with chromium (main cladding component):

$$Cs_2Te + Cr + 2O_2 \rightarrow Cs_2CrO_4 + Te$$

- Reaction with molybdenum (JOG component):

$$Cs_2Te + 2Mo + 7/2O_2 \rightarrow Cs_2Mo_2O_7 + Te$$

These reactions need oxygen potential higher than -400 kJ mol^{-1}, which are likely to occur at high burnup. The liberated tellurium reacts with clad constituents, forming iron and nickel tellurides:

$$Fe + 0.9Te \rightarrow FeTe_{0.9}$$

$$Ni + 0.6Te \rightarrow NiTe_{0.6}$$

2.03.5.3.4 Corrosion at fissile-fertile interface

A similar type of corrosion has also been observed at the upper end of the fissile column in front of the interface between fissile pellets and fertile pellets. Although localized and affecting a much smaller volume than the former type of FCCI, this localized corrosion may also reach locally similar depths, i.e., up to 200 μm. The mechanisms at work are probably the same as the previous type, but the local conditions are different: low fuel temperature with high oxygen potential, high clad temperature, and as cesium and tellurium reached this area after a long axial migration, their relative amounts may be quite different from their relative fission yield.

2.03.6 Cladding Failure

Although still under development, oxide fuel pins irradiated in fast reactors have demonstrated a high reliability, with a relatively small number of in-reactor clad failures (e.g., 15 pin failures with sodium ingress in Phénix for about 180,000 irradiated fuel pins ($<1.10^{-4}$), 23 failures in PFR, 12 in FFTF, out of 64,000 oxide fuel pins), most of them were experimental fuel pins.

In case of clad failure of an oxide fuel pin in sodium-cooled fast reactors, the first effect of the loss of tightness is a release of fission gases in the coolant. Reactors equipped with monitoring of fission gas above the coolant can detect this first stage of pin failure. The second step is sodium ingress inside the fuel pin, followed by an exchange of sodium between inside and outside the fuel pin. All fast reactors are equipped with a delayed neutron detector (DND), which detects the delayed neutrons released by some of the fission products escaping the fuel pin (For instance ^{96}Rb, ^{97}Rb, ^{89}Br…). This allows monitoring the evolution of the clad failure, as the DND signal is more or less related to the surface of fuel in contact with sodium. Some experimental and prototypic reactors have also used a gas-tagging system in order to detect failures and identify the responsible subassembly. In this method, a mixture of stable isotopes of a rare gas is added to the plenum of fuel pins, with different mixture for each subassembly.

The crucial point is the chemical incompatibility of mixed oxide and sodium. $(U, Pu)O_2$ reacts with sodium to form sodium uranoplutonate[55–58]:

$$3Na + (U, Pu)O_2 + O_2 \rightarrow Na_3(U, Pu)O_4$$

This reaction takes place at the periphery of the pellets (see an example in Fig. 19) and requires an oxygen supply.

As primary sodium coolant is very clean (1 or 2 ppm of oxygen), oxide fuel supplies the oxygen needed for the reaction. Consequently, the O/M ratio of the fuel decreases, and the reaction is stopped when the oxygen potential is low enough for the aforementioned reaction to reach equilibrium. For a low burnup fuel with a plutonium content of 20%, this O/M ratio equilibrium is about 1.96 at 750°C. The quantity of oxygen that can be supplied by the fuel and therefore the magnitude of the reaction increases both with plutonium content and with burnup. A stoichiometric UO_2 does not react with pure sodium, as there is no oxygen to feed the reaction. This has been verified experimentally on Phénix radial blanket pins.

Due to the radial temperature gradient, this reaction induces a radial migration of oxygen, which migrates down the thermal gradient. With an O/M ratio of about 1.96 at the limit between oxide fuel and the peripheral sodium uranoplutonate layer, the O/M ratio at the center of the pellet becomes very low, reaching values around 1.90.

When clad breaches occur at high burnup, the reaction progresses from the pellet periphery toward the pellet center by an intergranular front; the rate of oxide sodium reaction is higher at the grain boundary. The sodium uranoplutonate layer reaches a thickness of several hundreds of micrometers. The main consequences of this reaction are:

- An increase in fuel temperature due to the decrease of thermal conductivity induced by the decrease in O/M ratio. The sodium uranoplutonate layer also has a lower thermal conductivity than the oxide fuel (about a factor 3 lower),
- An increase in global fuel volume induced by the formation of uranoplutonate (which has a density about half the oxide density) and by the thermal expansion of oxide fuel due to reduction and subsequent heating of the fuel.

As a result of the reaction of sodium with the oxide fuel, the volume expansion of the fuel induces a strain in the cladding, with a risk of propagating the initial clad breach or developing a new breach; a secondary failure (Fig. 19). The sizes of primary and

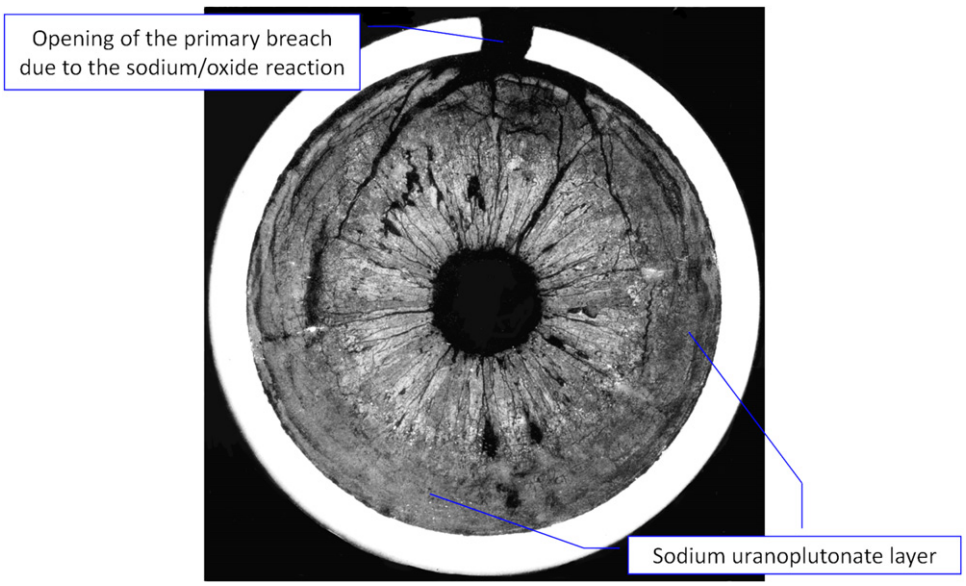

Fig. 19 Macrograph of a failed Phénix pin showing a wide layer of sodium uranoplutonate.

secondary failure depend greatly on the cause of the primary failure and of the residual ductility of the clad. Large clad failures (up to several hundreds of millimeters of axial extension) are found with embrittled clad materials.

The main consequence of clad failure is a release of fission products in the coolant; the fission gases that had been previously released in the pin plenum and a fraction of the volatile fission products such as cesium (typically 15%–40%). Cesium is soluble in sodium and sodium replaces cesium in most cesium compounds present in periphery (cesium uranates and molybdates). These releases of fission products not only depend upon the size of the failure but also on irradiation conditions; in particular, power variations induce a peak of fission product release by favoring sodium movements between inside and outside the fuel pin, and by modifying the fuel thermal regime.

Indeed, in most failure cases, there was no significant release of fissile material in the coolant. In practice, the fuel sodium reaction product was found to form a scab over the breach site, allowing operation in steady-state conditions for a considerable time without significant contamination of the primary coolant by actinide isotopes. But in order to guarantee they will avoid any release of fissile atoms, reactor operators have to determine a threshold of the DND signal beyond which the reactor is shut down and the subassembly with the failed pin is discharged. The time between DND failure detection and reactor scram may vary in a large range (from a few minutes to more than 100 days) depending upon the cause of rupture, the embrittlement of the clad, and the operating conditions. The shortest times have been observed in case of failure of high burnup rods, with brittle claddings occurring during power transients. This time is typically a question of hours or days, and generally the reactor has to be stopped before the next planned shutdown. This means that each pin failure causes a specific shutdown and stops the reactor for several days, the time needed to unload the failed subassembly and to load a new one.

The main consequences of fuel pin failures are, therefore, a pollution of the sodium coolant by radioactive nuclides and a decrease in the load factor of fast reactors. High reliability of fuel pins, with a failure rate of 10^{-5} or lower, is therefore a strong objective in the development of fast oxide fuel element.

2.03.7 Annular Pellets and Axially Heterogeneous Fuel Pin Concepts

2.03.7.1 Fuel Pins With Annular Pellets

The fuel pins designed for high-power fast reactors such as that used for Superphénix in the late 1970s, for the EFR Project in the late 1980s and, more recently, for the French Astrid Project, require an annular-shaped pellet of mixed uranium and plutonium oxide in order to:

- Maintain a sufficient margin with respect to fuel melting, particularly at the beginning-of-life when the fuel/cladding gap is still wide open,
- Provide a suitable low smear density ($<$ 85% TD) to achieve a target maximum burnup (15–20 at%) in accordance with the Generation IV requirements.

R&D on the SFR annular fuel pin concept in France has been particularly fruitful. The key objective of the major irradiation programs conducted in Rapsodie and Phénix[59] was to validate the annular fuel pin concept for Superphénix. No less than 1400 annular fuel pins were manufactured, loaded in sub-assemblies or in capsules, then irradiated up to burnup up to 12 at%. Furthermore, some of the pins from these annular fuel irradiation programs were subjected to safety tests as part of various safety programs on fast fuel elements carried out in the Cabri safety test reactor.

The analysis of feedback on the thermomechanical and physico-chemical behavior of annular fuel pins under nominal, incident and accident conditions led to the following conclusions:

The features of irradiated annular fuel are quite similar to that of solid fuel following its restructuring. Starting from the outer edge of the pellet, there is a non-restructured area close to the as-sintered microstructure, then an area with equiaxed grain growth, followed by a columnar grain zone and finally by a central hole whose manufacturing diameter has slightly increased (**Fig. 20**).

However, a small decrease of the as-manufactured central hole can be observed in pellets located near the bottom and top ends of the fissile column. This reduction in the size of the central hole is generally explained by a higher gaseous swelling of the fuel in these areas because of a rather high thermal regime due to a fuel/cladding gap remained open and polluted by fission gases.

A significant consequence of the thermal conditions encountered in annular pellet fuel pins is, at a given burnup, the fission gas release fraction of these fuel pins is close to those of the solid fuel pins.

Despite the limited data available at high burnup ($>$10 at%), it seems that, as for solid fuel pins, a JOG starts to form at a burnup in the range of 6–7 at%.

Non-destructive examinations and metallography cross-sections did not reveal any significant FCCI having occurred either at the beginning of irradiation (early-in-life corrosion) or at the end-of-life, particularly at the interface between the annular fuel column and the upper solid pellet UO_2 blanket. Nevertheless, this feedback remains insufficient in order to precisely determine the conditions under which FCCI occurs depending on operating parameters other than the burnup (linear heat rate, its time evolution and level of cladding temperature).

Though only based on a few provoked artificial failure tests, the behavior observed during a cladding failure seems to indicate that the additional volume available in the annular fuel pin could be advantageous for reducing the crack opening kinetics in the case of a chemical reaction with sodium.

Under incident and accident operating conditions, the respective impacts of a low smear density and a central hole in the pellet stack of the annular fuel pin, on the margin to a deterministic cladding failure during an inadvertent control rod withdrawal

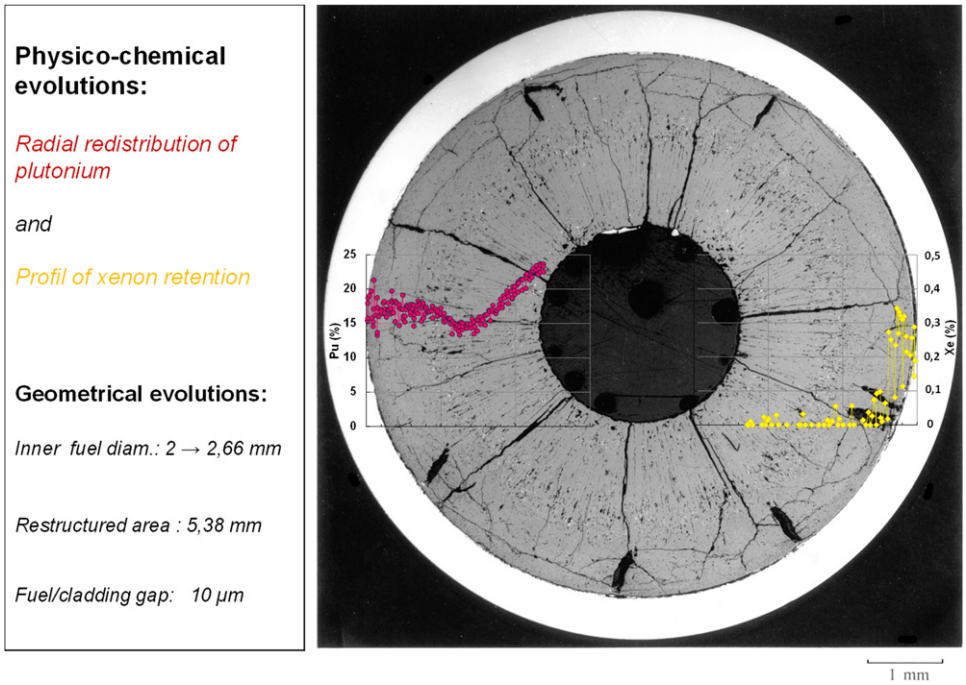

Fig. 20 Metallography showing the physico-chemical and geometrical evolutions of an annular fuel for a final burnup of 9 at%.

transient and on the enthalpy to failure in the case of a fast reactivity insertion, have been clearly demonstrated compared with similar tests performed on solid fuel pins. Therefore, annular fuel pins withstand the mechanical loads imposed during such transients much more efficiently than solid fuel pins.

2.03.7.2 Axially Heterogeneous Fuel Pin

The Axially Heterogeneous (Ax-Het) Cores for SFRs have been studied for several decades in the world. The consensus of these studies was that the Ax-Het core could provide improved nuclear performance and economic advantages. The main potential benefits of Ax-Het over homogeneous cores are an improved axial power form factor allowing an increase of the mean discharge burnup for a given peak burnup, a reduced dose over burnup ratio allowing a decrease of the damage on the cladding, an increased breeding ratio and last but not least, as part of the intrinsic safety improvement, a positive impact of this concept in reducing the sodium void effect.[7]

So, a certain number of experiments on axial heterogeneous fuel pin concept were conducted until the final shut down of Phénix in 2009 representing more than 2000 Ax-Het pins irradiated in the Zèbre and Pavix programs.

Fig. 21 shows the diagram of a typical axial heterogeneous fuel pin completed by the axial profile of its linear heat rate (LHR) in the fissile and fertile zones at the beginning (continuous line) and at the end of irradiation (dashed line).

During irradiation, the LHR of the two fissile zones with an initial plutonium content of about 28% decreases while that of the fertile zones increases, especially for the internal blanket for which the LHR more than double at the end of irradiation. As a result, the very large initial variations of power at the various fissile/fertile interfaces tend to be gradually reduced with the burnup.

Of course, these axial power singularities affect the cladding with significant variations in temperature and temperature gradient in the cladding thickness at the two main interfaces separating the internal blanket from the low and high fissile columns. In case of cladding swelling, these temperature anomalies lead to localized strains of a few tens of microns at the lower fissile/internal blanket interface. Nevertheless, this extra deformation does not affect the mechanical behavior of the pin.

On the basis of the post-irradiation examinations, the thermal behavior of the fissile zones of the heterogeneous pin is consistent with the irradiation parameters and quite similar to that of homogeneous pins at same burnup and identical cladding deformation. At high burnup, the cesium is partly removed from the fuel and together with other fission products constitutes a JOG. The compounds present in this JOG appear of the same nature as in the homogeneous pins.[60]

Concerning the internal blanket, for highly irradiated Ax-Het pin, the thermal regime of the UO_2 pellets may be characterized by an unfinished restructuring that can go as far as the beginning of central hole formation accompanied by a very important release of the fission gases (>50%) according to its own dissipated power. This behavior is consistent with the fact that the pellet to cladding gap remains open but becomes particularly polluted in fission gases (Xe + Kr) owing to the high release that comes from the fissile columns.

It appears that the presence of this internal blanket, leads to a very clear decoupling between the lower and the upper fissile columns. This constitutes an essential difference between the concepts of homogeneous and heterogeneous fuel pins.

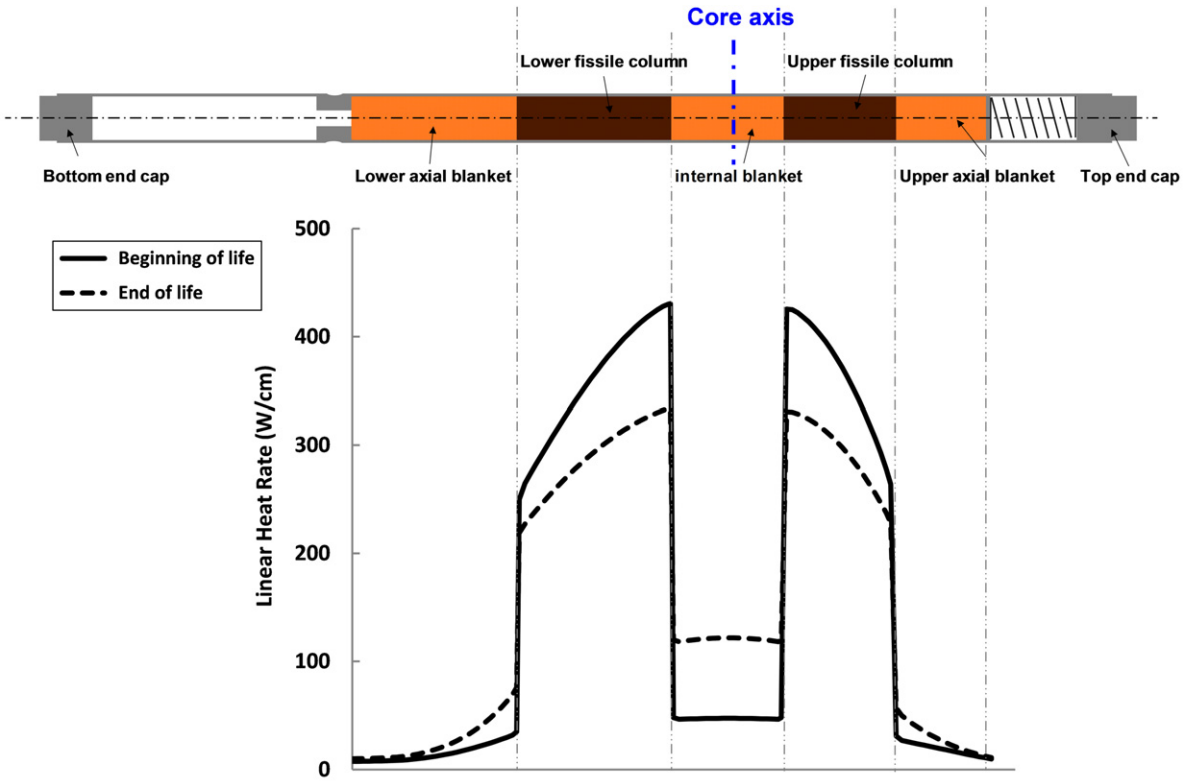

Fig. 21 Diagram of an axial heterogeneous fuel pin (Zèbre type) and axial distribution of the LHR at beginning and end of life.

The observations on heterogeneous pins have been reassuring regarding the internal blanket/fissile interfaces:

- Measurements by EPMA clearly showed that the axial plutonium diffusion remains very limited in adjacent breeder pellets (<200 μm) (Fig. 22),
- γ-scanning indicated that there was no axial transfer of cesium from one side of the internal blanket to the other, the two fissile columns being ignored from this point of view.

The limited FCCI which was observed on a significant number of Ax-Het pins may be linked to the decoupling, induced by the internal blanket, as has been demonstrated at the level of the fuel to cladding interface. For this, we must refer (see Section 2.03.5.3.3) to the mechanisms put forward to explain the strong FCCIs of homogeneous fuel pins with a clad made of stabilized austenitic steel: when this material starts to swell, the cladding strain in the lower half of the fissile column would cause, through the overheating of the associated fuel, an axial migration of the upwardly corroding fission products, an increase in the oxygen potential of the oxide and an axial migration of oxygen, contributing to the meeting of favorable conditions for inner cladding corrosion in the upper half of the fissile column. The decoupling found in the Ax-Het pin concept is such as to alter the axial migration of the volatile fission products and modify the thermodynamic conditions along the pin, so that the conditions for a strong FCCI in the upper fissile column are no longer imposed by what happens in the lower fissile column.

In conclusion, these experiments on Ax-Het fuel pins clearly demonstrated:

- An absence of deleterious effects in the internal blanket zone, particularly at the fissile/internal blanket interfaces suggesting that the life limiting features identified for an Ax-Het pin are not more severe, or even less, than for a homogeneous fuel pin,
- A significant reduction of the FCCI depth for pins irradiated in similar conditions in terms of LHR and burnup compared to homogeneous pins.

2.03.8 Summary and Outlook

Oxide fuel for fast reactors has proved to be a mature, quite reliable, and very robust fuel concept. The low conductivity of mixed oxide may appear as a weakness of this fuel as it induces a limitation of linear heat generation. However, thanks to its high operating temperature and related high creep rate, fuel mechanical loadings to the cladding remain low, and oxide fuel pins have demonstrated an ability to reach extremely high burnup.

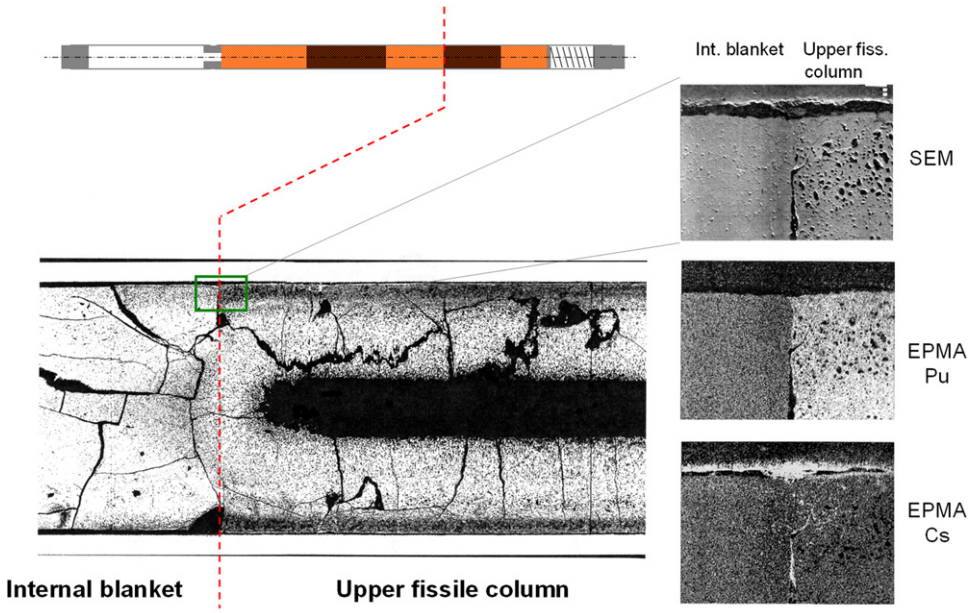

Fig. 22 Axial optical macrograph and details from scanning electron microscope and microprobe analysis clearly showing the absence of plutonium diffusion toward the internal blanket.

Experience achieved in the past decades on oxide fuel behavior in fast reactors paves the way to face the new challenges of the next generation of reactors for Generation IV systems. Even if other types of fuel (such as carbide, nitride, or metals) are also considered, if advantages and drawbacks of the different fuels are still weighed, it is likely that the first prototypes of this new generation which are currently built in China, India and Russian federation will use oxide as it is the most mature fuel among the various candidates.

All phenomena occurring in fast oxide fuel during its irradiation are relatively well understood and modeled. However, it might be useful in the future to improve the accuracy of fuel performance code predictions, in particular regarding the thermal margin to fuel melting at high burnup or the consequences of extended FCCI. This will imply developing quantitative modeling of thermochemical phenomena, such as JOG formation or clad inner corrosion, which may be quite complex as these mechanisms involve not only thermodynamics but also considerable radial and axial transport of a great number of fission product compounds.

Acknowledgment

The authors wish to thank J. Noirot (CEA) and N. Chauvin (CEA) for the critical review of the manuscript.

See also: 2.06 Thermal Properties of Irradiated UO_2 and MOX. 2.08 Matter Transport in Fast Reactor Fuels. 2.12 Behavior of Fast Reactor Fuel During Transient and Accident Conditions. 2.13 Oxide Fuel Performance Modeling and Simulation. 3.02 Radiation-Induced Damage in Austenitic Structural Steels Used in Nuclear Reactors. 3.05 Radiation Effects in Ferritic Steels and Advanced Ferritic-Martensitic Steels. 3.06 Oxide Dispersion Strengthened Steels. 7.03 Thermodynamic and Thermophysical Properties of the Actinide Oxides. 7.15 Thermophysical Properties of Liquid Metal Coolants: Na, Pb, Pb–Bi(e)

References

1. Olander, D.R., 1976. Fundamental aspect of nuclear reactor fuel elements. Report no.TID-26711-P1, TN.
2. Lambert, J.D.B., Strain, R., 1994. In: Frost, B.R.T. (Ed.), Materials Science and Technology, Volume 10 A – Nuclear Materials. New York: VCH, pp. 108–190.
3. Guérin, Y., 1999. The nuclear fuel of pressurized water reactors and fast reactors. In: Bailly, H., Ménessier, D., Prunier, C. (Eds.), Collection du Commissariat à l'Energie Atomique. Paris: Lavoisier, pp. 77–158.
4. Millet, P., Ratier, J.L., Ravenet, A., Truffert, J., 1999. The nuclear fuel of pressurized water reactors and fast reactors. In: Bailly, H., Ménessier, D., Prunier, C. (Eds.), Collection du Commissariat à l'Energie Atomique. Paris: Lavoisier, pp. 437–529.
5. Martin, P., Pelletier, M., Every, D., Buckthorpe, D., 2008. French and United Kingdom experience of high-burnup mixed-oxide fuel in sodium-cooled fast breeder reactors. Nucl. Technol. 161, 35–43.
6. Pelletier, M., 2009. The Phénix Reactor, Assessement of 35 Years' Operation – Revue Générale Nucléaire no.1 Janvier – Février, pp. 34–41.

7. Pages, J.P., Brown, C., Steinmetz, B., Languille, A., 1991. Chapter 6.2.1 – Development of the axially heterogeneous fuel concept in Europe. In: Proceedings of the International Conference on Fast Reactors and Related Fuel Cycles, vol. 1, Kyoto, Japan.
8. Gratchyov, A.F., Skiba, O.V., Tsykanov, V.A., *et al.*, 2007. Demonstration experiment of 3 BN-600 MOX vibropac FAs irradiation for the excess weapons plutonium disposal. J. Nucl. Sci. Technol. 44 (3), 504–510.
9. Conte, M., Gatesoupe, J.P., Trotabas, M., Boivineau, J.C., Cosoli, G., 1979. Study of the thermal behaviour of LMFBR fuel. In: Proceedings of the International Conference Fast Breeder Reactor Fuel Performance, pp. 301–319. Monterey.
10. Rand, M.H., Roberts, L.E.J., 1965. Proceedings of Symposiumin in Thermodynamics, vol. 1, Vienna: IAEA. STI/PUB/109.
11. Rand, M.H., Markin, T.L., 1967. Proceedings of a Symposium on the Thermodynamics of Nuclear Materials (IAEA. STI/PUB/162). Vienna.
12. Aitken, E.A., 1969. J. Nucl. Mater. 30–62.
13. Bober, M., Schumacher, G., 1973. Adv. Nucl. Sci. Technol. 7, 495–564.
14. Sari, C., Schumacher, G., 1976. J. Nucl. Mater. 61, 192–202.
15. Tanaka, K., Miwa, S., Sato, I., *et al.*, 2009. J. Nucl. Mater. 385, 407–412.
16. Olander, D., 1973. J. Nucl. Mater. 49, 21–44.
17. Clement, C.F., Finnis, M.W., 1978. J. Nucl. Mater. 75, 193–200.
18. Guarro, S., Olander, D.R., 1975. J. Nucl. Mater. 57, 136–144.
19. WPFC Expert Group on Innovative Fuels, 2012. Homogeneous versus Heterogeneous Recycling of Transuranics in Fast Nuclear Reactors. Nuclear Energy Agency. (NEA no. 7077 OECD ISBN 978-92-64-99177-4).
20. Maeda, K., Sasaki, S., Kato, M., Kihara, Y., 2009. J. Nucl. Mater. 385, 413–418.
21. Kleykamp, H., 1985. J. Nucl. Mater. 131, 221–246.
22. Lindemer, T.B., Besman, T.M., Johnson, T.E., 1981. J. Nucl. Mater. 100, 178–226.
23. Adamson, M.G., Aitken, E.A., Lindemer, T.B., 1985. J. Nucl. Mater. 130, 375–392.
24. Kleykamp, H., Paschoal, J.O., Pejsa, R., Thummler, F., 1985. J. Nucl. Mater. 130, 426.
25. Tourasse, M., Boidron, M., Pasquet, B., 1992. Effect of clad strain on fission product chemistry in Phénix pins at high burnup. In: Proceedings of the Symposium on Materials Chemistry '92', p. 13, Tsukuba.
26. Sato, I., Furuya, H., Arima, T., Idemitsu, K., Yamamoto, K., 1999. J. Nucl. Mater. 273, 239–247.
27. Matzke, H.J., Ottaviani, J.P., Pellotiero, D., Rouault, J., 1988. J. Nucl. Mater. 160, 142–146.
28. Inoue, M., Maeda, K., Katsuyama, K., Mondo, K., Hisada, M., 2004. J. Nucl. Mater. 326, 59–73.
29. Tourasse, M., Boidron, M., Pasquet, B., 1992. J. Nucl. Mater. 188, 49–57.
30. Maeda, K., Tanaka, K., Asaga, T., Furuya, H., 2005. J. Nucl. Mater. 344, 274–280.
31. Ishii, T., Mizuno, T., 1997. J. Nucl. Mater. 247, 82–85.
32. Maeda, K., Asaga, T., 2004. J. Nucl. Mater. 327, 1–10.
33. Roche, L., Pelletier, M., 1999. Modeling of the thermomechanical and physical processes in FR fuel pins using the Germinal code. In: Proceedings of the International Symposium on MOX Fuel Cycle Technologies for Medium and Long-Term Deployment (IAEA-SM-358/25), May 1999, pp. 17–21. Vienna, Austria.
34. Maeda, K., Katsuyama, K., Asaga, T., 2005. J. Nucl. Mater. 346, 244–252.
35. Noirot, J., Desgranges, L., Lamontagne, J., 2008. J. Nucl. Mater. 372, 318–339.
36. Teague, M., Gorman, B., King, J., Porter, D., Hayes, S., 2013. J. Nucl. Mater. 441, 267–273.
37. Teague, M., Gorman, B., Miller, B., King, J., 2014. J. Nucl. Mater. 444, 475–480.
38. Zimmermann, H., 1979. Fission gas behavior in nuclear fuels, European Applied Research Report, vol. 1 (1), pp. 127–138. Harwood: London.
39. Dubuisson, P., De Carlan, Y., Garat, V., Blat, M., 2012. J. Nucl. Mater. 428, 6–12.
40. Baker, R.B., Legett, R.D., 1979. Proceedings of the International Conference on Fast Breeder Reactor Fuel Performance, p. 258. ANS: La Grange Park, IL.
41. Renault, C., Rouault, J., Anzieu, P., 2009. Status and perspective of fuel developments for fast neutron reactors of 4th generation. In: Proceedings of the RRFM International Conference.
42. Mélis, J.C., Piron, J.P., Roche, L., 1993. J. Nucl. Mater. 204, 188–193.
43. Gatesoupe, J.P., Guérin, Y., Courtois, C., Truffert, J., 1979. Fuel cladding mechanical interaction – Observation and analysis. In: Proceedings of the International Conference Fast Breeder Reactor Fuel Performance, pp. 246–257. Monterey.
44. Biancheria, A., Roth, T.S., Nayak, U.P., Boltax, A., 1979. Fuel-cladding mechanical interaction in fast reactor fuel rods. In: Proceedings of the International Conference Fast Breeder Reactor Fuel Performance, pp. 513–535. Monterey.
45. Levine, P.J., Nayak, U.P., Schwallie, A.L., Boltax, A., 1979. Irradiation performance of WSA-3, -4, and-8 mixed-oxide fuel pins in grid-spaced assemblies. In: Proceedings of the International Conference Fast Breeder Reactor Fuel Performance, pp. 143–154. Monterey.
46. Dienst, W., Guérin, Y., Gatesoupe, J.P., Müller-Lyda, I., 1980. Journal of Nuclear Materials 91, 73–84.
47. Naganuma, M., Koyama, S., Asaga, T., *et al.*, 1999. High burnup irradiation performance of annular fuel pins irradiated in fast reactor PFR (IAEA-SM-358/24). In: Proceedings of the International Symposium on MOX Fuel Cycle Technologies for Medium and Long-Term Deployment, May 1999, pp. 17–21. Vienna, Austria.
48. Fee, D.C., Johnson, C.E., 1981. J. Nucl. Mater. 99, 107–116.
49. Adamson, M.G., Aitken, E.A., 1985. J. Nucl. Mater. 132, 160–166.
50. Pulham, R.J., Richards, M.W., 1990. J. Nucl. Mater. 171, 319–326.
51. Götzmann, O., 1990. Proceedings of the BNES Conference on Fast Reactor Core and Fuel Structural Behavior, pp. 1–8. London.
52. Yates, G., Linekar, G.A.B., 1987. Fuel/clad chemical interaction in PFR fuel pins. In: Proceedings of the International Conference on Materials for Nuclear Reactor Core Applications, Oct 1987, pp. 329–333. Bristol: BNES.
53. Ratier, J.L., 1992. Phénomènes de corrosion des gaines d'éléments combustibles de réacteurs à neutrons rapides. In: Proceedings of the EUROCORR Conference, June 4, 1992. Espoo, Finland.
54. Ball, R.G.J., Burns, W.G., Henshaw, J., Mignanelli, M.A., Potter, P.E., 1989. J. Nucl. Mater. 167, 191–204.
55. Mignanelli, M.A., Potter, P.E.J., 1984. J. Nucl. Mater. 125, 182.
56. Lorenzelli, R., Athanassiadis, T., Pascard, R., 1985. J. Nucl. Mater. 130, 298.
57. Pillon, S., 1989. Etude des diagrammes de phases U–O–Na et U, Pu–O–Na. Thesis Université des Sciences et Techniques du Languedoc. Rapport CEA-R-5489.
58. Kleykamp, H., 1990. Assessment of the physico-chemical properties of phases in the Na–U–Pu–O system. Kernforschungszentrum Karlsruhe report, KFK 4701.
59. Pelletier, M., Pillon, S., Fontaine, B., Seran, J.L., 2009. The Phénix Reactor – Assessement of 35 Years' Operation Revue Générale Nucléaire no.1 Janvier–Février, pp. 94–110.
60. Boidron, M., Berlanga, C., 1986. Pile Behavior of Axially Heterogeneous Fuel Elements in International Conference on Reliable Fuels for Liquid Metal Reactors, September 7/11, 1986. ANS: Tucson.